# MODELLING OF TWIN-AXES TABLE DRIVE SYSTEM

LIM VUN HAW



**BACHELOR OF MECHATRONICS ENGINEERING**

**UNIVERSITI TEKNIKAL MALAYSIA MELAKA**

“I hereby declare that I have read through this report entitled “ Modelling of Twin-Axes Table Drive System” and found that it complies the partial fulfilment for awarding the degree of Bachelor of Mechatronics Engineering”.

Signature : ______________________________

Supervisor‟s Name : ______________________________

Date : ______________________________

**MODELLING OF TWIN-AXES TABLE DRIVE SYSTEM**

**LIM VUN HAW**

**A report submitted in partial fulfilment of the requirements for the degree of**

**Mechatronics Engineering**



**Faculty of Electric Engineering**

**UNIVERSITI TEKNIKAL MALAYSIA MELAKA**

**2017/2018**

I declare that this report entitled "Modelling of Twin-Axes Table Drive System" is the result of my own research except as cited in the references. The report has not been accepted for any degree and is not concurrently submitted in candidature of any other degree.

Signature : ______________________________

Name : ______________________________

Date : ______________________________

To my beloved mother and father

## ACKNOWLEDGEMENT

First and foremost, I wish to express my greatest appreciation and deepest gratitude to my supervisor, AINAIN NUR BINTI HANAFI for constantly guiding and encouraging me throughout the entirety of this final year project. Thank you for giving me valuable advice and suggestion to bring this report to its final form. Without her support and interest, this report would not have been the same as presented here. I am very grateful for her patience and constructive comments that enriched this FYP.

I am also grateful to PROFESSOR MADYA DR. CHONG SHIN HORNG, for her provision of expertise in the implementation. She guided my throughout the implementation process from designing, fabrication until implementation. Improvements are done on the all the stages to obtain a better performance by looked into details the overlooked matters. Without her superior knowledge and experience, the FYP project wouldn‟t like in quality of outcomes.

In particular, my sincerely gratitude is also extends to all of my friends for their generous efforts and assistances provided in enlightening me. Their views and tips are useful indeed. I would like to acknowledge their comments and suggestions, which was crucial for the successful completion of this project. Also, I would take this opportunity to express my gratitude to my parent for their continuous shower of love, unceasing encouragement and support throughout all these years.

Last but not least, I place on record, my sense of gratitude to one and all who, directly or indirectly, have offered their helping hand during the entire period of final year project.

# ABSTRACT

Table Drive System is commonly used in industrial sectors to transfer load from one place to another place. As load weight increases, different types of tables actuated by a number of motors are developed to sustain the increase in workload. Twin-axes Table Drive System (TTDS) is constructed in this report. The TTDS has two similar units of single axis ball screw jointed together with a large mover. Two DC servo motors produce input torque with rotary motion to the TTDS. This report is also presented system modelling technique for twin axes table drive system through simulation. The table of two ball screws and motors are attached with an aluminium bar where each end of the bar is attached firmly to the slide mover. This configuration aims to sustain the increase in weight to be driven. However, synchronization of two coupled parallel ball screws is a major problem. The block diagram of the twin axes table drive system (TTDS) is constructed from past research. Hence, system identification technique is performed to construct mathematical model of the twin axes table drive system via frequency response through simulation. The transfer function obtained can present the simulated system. The performance of the twin axes table drive system is compared to the single axis ball screw table in term of load weight to be driven using Simscape. Result showed that the TTDS has better performance for 2 kg to 10kg load as compared to single axis ball screw system.

# ABSTRAK

Sistem Pemanduan Meja lazimnya digunakan dalam sektor industri untuk memindahkan beban dari satu tempat ke tempat lain. Dengan peningkatan berat beban, pelbagai jenis pemanduan meja yang beroperasi dengan motor dibangunkan bagi menyokong peningkatan beban kerja. Sistem Pemacu Meja Kapak Kembar (TTDS) dibina dalam laporan ini. TTDS mempunyai dua unit serupa paksi bola paksi tunggal bersatu bersama penggerak besar. Dua motor servo DC menghasilkan tork masukkan dengan gerakan putar pada TTDS. Laporan in juga memperkenalkan prosedure sistem identifikasi untuk TTDS melalui simulasi. TTDS yang mengandungi dua motor dan dua unit skru bola telah dilampirkan dengan bar aluminium di tepi meja pegerakan. Konfigurasi ini mampu meningkatkan keupayaan TTDS untuk menangkat beben yang lebih berat. Akan tetapi, masalah bersegelarah masih menjadi masalah besar untuk TTDS. Oleh itu, teknik sistem identificasi diaplikasikan untuk mendapatkan fungsi pemindahan TTDS melalui simulasi. Rangkap pindah yang diperoleh dapat memberikan melaksanakan fungsi yang serupa dengan sistem rujukan. Pelaksanaan antara TTDS dengan sistem pemacu meja satu paksi dibandingkan dengan mengakat beban yang berlainan melalui Simscape. Keputusan menunjukkan bahawa TTDS mempunyai pelaksanaan yang lebih baik daripada sistem pemacu meja satu paksi bagi 2 kg sehingga 10 kg beban.

# TABLE OF CONTENTS

# LIST OF TABLES

# LIST OF FIGURES

# LIST OF APPENDICES

# CHAPTER 1

# INTRODUCTION

## 1.1 Overview

This chapter presents the motivation, problem statement, objective, and scope of the proposed project.

## 1.2 Motivation

Malaysia was one of the few countries that swam against the tide during the deindustrialization in late of 1990s. Manufacturing shares in Malaysia‟s manufactured goods have risen from 25% in early 1980s to 80% in 2012 [1]. This statement showed that the increased in amount of manufacturing sector over these decades. The growth in manufacturing is expected to increase over the year until year 2020 based on Figure 1.1.

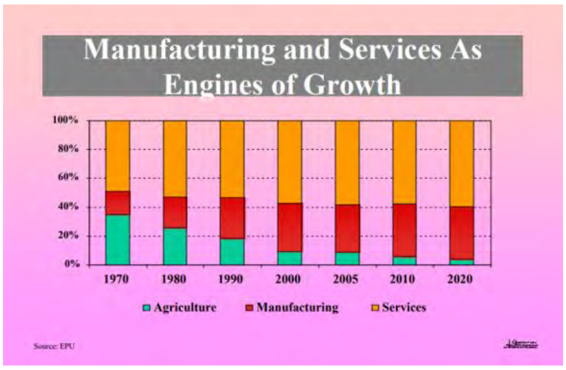


Figure 1.1: Manufacturing and Services as Engines of Growth [2]

With the increases in manufacturing sector, the demands on machines will also increases to maximize the productivity. This will lead to the increase of weight driven in corresponding to productivity.

In machine tool and semiconductor manufacture fields for examples machining centre, a semiconductor photolithography machine, and others [3], the need for high precision and fast response time in numerical control machine is rapidly growing [4]. As the load weight to be driven increases, multiple axis table drive system is in demand.

Twin-axes table drive system (TTDS) is installed with multiple motors which move in same direction simultaneously. The use of multiple motors generates high power for heavy duty tasks with low cost.

## 1.3 Problem Statement

Research on the TTDS has received a lot of attention. The previously technology is single ball screw system which is unable to sustain the increase of the load weight to be driven. Another innovation of this system is needed to address the demand of the industrial growth.

This innovation has led to the development of different types of synchronous to compensate the synchronisation error of the TTDS. Asynchronous motion of the each axis leads to the damage of the drive system. On the other hand, the existence of the synchronous error of both mechanically coupled twin drives remains the main problem. This error is caused by the characteristics of the drive system. Friction and other disturbances as well, prevent the system to achieve the desired performance. In order to compensate these errors, the system‟s characteristics need to be well understood. The system‟s characteristics define by a transfer function can be obtained using the modelling technique. This model of the system‟s characteristics needs to be verified to ensure the error is within the acceptable range.

Besides, the performance of the TTDS is concerned by all the parties involved. The performance of the system is a crucial for the productivity. The replacement of the new system is required to compare with the old system, single ball screw system in term of capability to drive load.

## 1.4 Objectives

The aims of the Final year Project (FYP) are:

1) To design and develop a twin-axes table drive system (TTDS), which is driven by DC servo motors with ball screws.
2) To model the dynamic characteristics of the twin-axes table drive system (TTDS) via frequency response method through simulation.
3) To validate the transfer function via simulation.
4) To compare the performance of single axis ball screw and twin-axes table drive system (TTDS) with varying load via Simscape.

## 1.5 Scope

The extents of the area of TTDS are:

1) This system is installed with two units of:
   a) DC servo motors: 30VDC
   b) Linear encoder: 5um.
   c) Linear guides
2) Both axes have a mover that joint together via a longer mover.
3) The mover motion is in either forward or backward direction.
4) The maximum load weight to be driven by this system is 10Kg.
5) The modelling and performance comparison of TTDS is conducted via simulation

## 1.6 Report Outline

Chapter 2 covers the basic principle of twin-axis table drive system which consists of motor and ball screw. Reviews of previous related works and evaluation on control methods are also presented.

Chapter 3 discusses the methodology to accomplish the objectives of the project. Explanations on the selected components and related experiments are described to ensure the attainment of the objectives. These details include the procedures used.

The results are presented in Chapter 4. Design of the TTDS is illustrated using SolidWorks with the stress test on large mover. The mathematical modelling and performance comparison of TTDS is obtained using Matlab. Chapter 5 provides the summary and suggestion for future works for the proposed project.

# CHAPTER 2

# LITERATURE REVIEW

## 2.1 Overview

Basic working principal of TTDS and types of motor will be presented in this chapter. In order for the TTDS to perform better, single loop controllers are discussed. Different types of synchronous control methods are reviewed in order to control the motion of both axes. Reviews on previous works related to twin-axes table drive system from different journals or conference papers are presented. Evaluation is done based on the previous works.

## 2.2 Twin-Axes Table Drive System

The usage of dual-stage system started since late 1980s. Dual-stage system is defined as a combination of coarse and fine stages whereby each stage is driven by a coarse actuator and fine actuator respectively [5]. [6] proposed two drive units arrange to form a single feed axis in modern gantry type configurations. Such drive units has the potential applications in wave makers, machining tools, large sized liquid crystal panel producer machine, and others. Recently, commonly used driven stages in industrials are ball screw driven stage and linear motor driven stage. Both types of stage are synchronised with synchronous control. Types of synchronous controls used are cross-coupling motion control, master-slave motion control and relatively dynamics stiffness motion control [7]. Different single loop controls are introduced before the introduction of synchronous motion control.

### 2.2.1 Ball screw driven stage

In earlier days, hydraulic actuators are used in positioning applications, but require many valuable hours of testing and maintenance [8]. Piezoelectric Actuators (PAs) are used to replace hydraulic actuators in the application of micro positioning. However, this actuator has limited displacement application where the size of PAs increases for long distance application and result in increase of driving voltage. This problem leads to the implementation of ball screw actuator by servo motor. Servo motor is capable of ensuring precise control of angular or linear position.

The common configuration of single ball screw drive used is shown in Figure 2.1, where the mover slides along with one or more linear guides. The linear motion is generated by ball screw with servo motor [9].

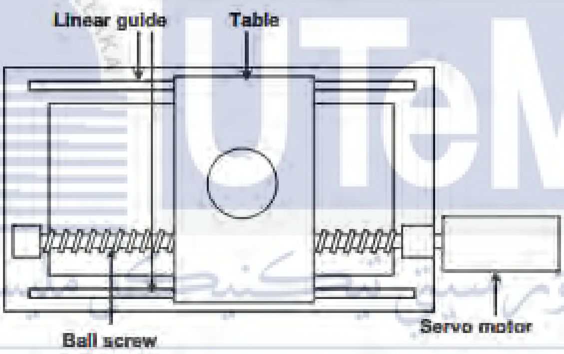


Figure 2.1: Single ball screw drive stage [9]



A servo motor operates in rotary motion, requires a linear motion translator. The ball screw translates rotational motion to linear motion with little friction. Additional mechanism of linear guide is also required to ensure the motion of the mover remains in straight line. A positioning control of both type of drive system is dependent on position detector [10] such as linear encoder.

This configuration is capable in achieving satisfactory accuracy. In recent development, improvements are made in term of work piece scale. Larger ball screw driven stages are recommended to drive greater load weight. This condition has resulted in large spans between linear guides of stages and may reduce the accuracy due to the occurrence of skewed.

[9] proposed the solution to drive the mover of a large single feed axis with two ball screws and motors which provide a joint thrust for driving the large mover as shown in Figure 2.2. [11] also proposed the use of parallel drive mechanism of ball screw to replace the oil pressure drive system with injection moulding machine. The high stiffness, high transmission accuracy and low sensitive to variation in working with cutting force and workpiece mass make ball screw the preferable machine used in industries [12, 13].

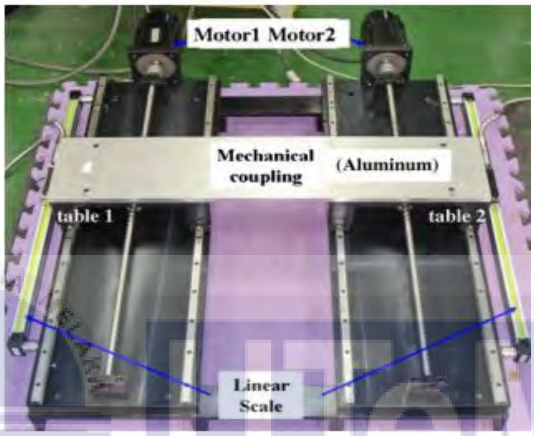


Figure 2.2: Twin ball screw drive system [9]

Drive mechanism of ball screw and servo motor consumes less power than oil pressure drive mechanism. However, such application requires large diameter of ball screw and limits the rotation speed. It is necessary to use multiple motors with smaller diameter of ball screw to achieve desired injection speed as shown in Figure 2.3.

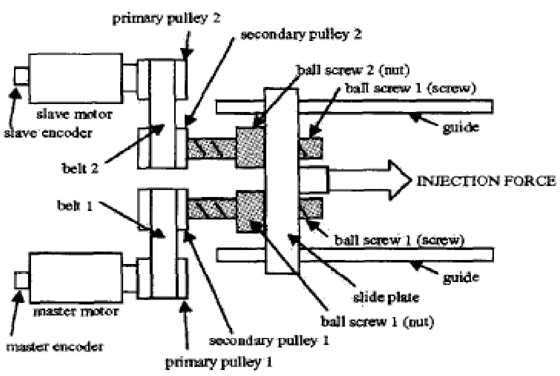


Figure 2.3: Parallel ball screw drive system [11]

From the reviews, servo motor is favourable for ball screw drive system [9], [14]. Servo motor has built-in rotary encoder which can detect rotational angle and angular speed of the motor. This feature allows feedback to controller for better controlling purpose.

### 2.2.2 Linear Motor Drive Stage

Linear motor is latest technology of motor and has been applied to actuate drive stage [7] as shown in Figure 2.4.

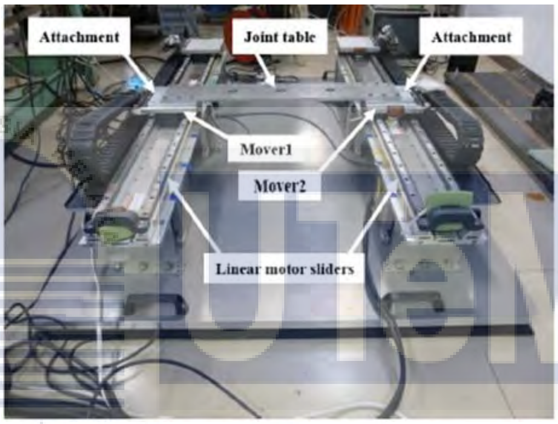


Figure 2.4: Twin linear motor drive system [7]



In general, linear motor and rotary motor has the same working principle. A linear motor is produced when a rotary motor is split and stretch in plane as shown in Figure 2.5.

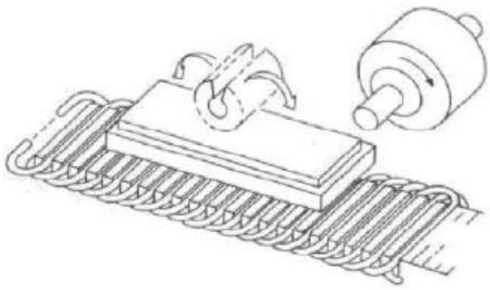

Figure 2.5: Structural similarity of linear motor to rotary motor [15]

Motor converts electric current directly to mechanical power base on the Lorentz force law. Lorentz force law is defined as an induced force applied to a current carrying conductor in the present of magnetic field. A simple explanation on the operation of linear motor is that current flows through a wire and the direction of flow is perpendicular to the magnetic field. An induced force results in wire will produce motion. The direction and magnitude of current, magnetic field and angle between current and magnetic field will affect the magnitude of induced force.

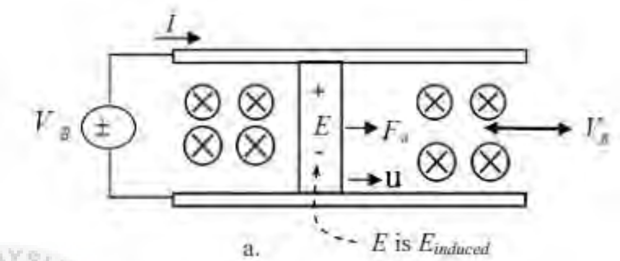


Figure 2.6: Linear mechanism [16]

The force induced by linear motor is independent of magnetic field and moving point charge. Such relationship can be computed by Lorentz‟s force equation by (2.1).

$$\boldsymbol{F = q(v \times B)} \tag{2.1}$$



where $q$ is the charge, $v$ is the velocity of the mover, $\boldsymbol{B}$ is the magnetic flux density acting on the mover, and x denotes the vector cross product of velocity and flux density. While

$$\boldsymbol{qv = il} \tag{2.2}$$

Lorentz‟s force can be expressed as in equation (2.3).

$$\boldsymbol{F = i(l \times B_g)} \tag{2.3}$$

where $\boldsymbol{F}$ is the electromagnetic force vector, $\boldsymbol{l}$ is the vector of magnitude l in the direction if current i and $\boldsymbol{B_g}$ is the air-gap magnetic flux density vector, and x denotes the vector cross product. The magnitude of the resulting force can be rewritten with the definition of cross product as in equation (2.4).

$$\boldsymbol{F = B_g\ li\ sin\alpha} \tag{2.4}$$

where α is the angle between l and $\boldsymbol{B_g}$ vectors. Left-hand rule is used to determine the direction of induced force. Maximum force produces when $\boldsymbol{l}$ and $\boldsymbol{B_g}$ are orthogonal whereby α = π/2. Base on the relationship, force produced can be given in equation (2.5).

$$\boldsymbol{F = B_g\ li = k_f\ i} \tag{2.5}$$

where $\boldsymbol{k_f}$ is the force constant in newton per ampere (N/A). Faraday‟s law of electromagnetic induction is implied voltage (EMF) U same as Lentz‟s law which induced in a conductor moving with a velocity $\boldsymbol{v}$ in the present of magnetic flux density $\boldsymbol{B_g}$, the induced voltage is expressed in equation (2.6).

$$\boldsymbol{U = B_g\ lv = k_e v} \tag{2.6}$$

where $\boldsymbol{k_e}$ is the voltage constant in volt-second per metre (Vs/m) and $\boldsymbol{v}$ is the velocity in metre per second (m/s). Right-hand rule is used to determine the direction of induced voltage. Note that $\boldsymbol{k_f}$ and $\boldsymbol{k_e}$ are numerically equal when SI units are used [17].

Different types of linear motors are used to manufacture TTDS. There are two types of linear motors; DC linear motor and AC linear motor. The control and structure of linear DC motor are simpler than the linear AC motor. The influence of loading motor on stiffness test can be reduce due to low thrust ripple of linear DC motor [18].



On the other hand, linear asynchronous (induction) motor is widely used due to the conducting sheet requires no power supply and little maintenance. Application of linear induction motor is in small factory due to low positioning accuracy. The high demands on electronic control have shifted interest in linear stepping motors and linear DC motor because of precise linear movement. However, there is possibility in linear steeping motors of failure or step-out due to overloads and disturbances exits if no encoder facility is used. An additional position control loop is required if the current position accuracy afforded by slotting is insufficient. Such additional is considered costly, in comparison with linear DC motors whereby the positioning control is dependent on the position detector [17].

### 2.2.3 Single Axis Controller Design

To enhance the dynamic performance of the TTDS, there are two aspects should be considered carefully [19]. First aspect is the high response of position tracking of each axis, and second aspect is the high respond in reducing synchronous error of position with dual linear motors. Only the first aspect will be discussed in this section. The other aspect will be discussed later in section 2.2.5.

From previous researches, there are several types of controllers used such as PID, Fuzzy logic controller, and feed forward controller. [20] proposed fuzzy PID in controlling dual linear motor. A conventional controller of PID can be considered as a form of phase lead-lag compensator with one pole near origin and the other at infinity. PI and PD are in the same family as PID controller. Each letter has different functionalities [20].

P, Proportional means to fasten the response speed of the system; determine s respond to current error, providing overall control action proportional to error signal. I, Integral is used to reduce steady state error by an integrator, determines reaction based on sum of errors whereas, D, Derivative improves transient respond by differentiator, determines reaction based on rate of errors.

Fuzzy-logic controller (FLC) is designed to follow standard design procedure or fuzzy rule which consists of fuzzification of input values, fuzzy inference, and defuzzification of output. Fuzzy rules and reasoning are utilized on-line to decide the controller parameter based on error signal and error rate [19,20]. Fuzzy controller has good robustness and dynamics property but indelibility in static error. However, PID controller can eliminate static error but poor in dynamics respond. Thus, the hybrid of these both controllers can achieve better performance which leads to the intensively application in various fields [20].

As for feed forward controller, the principle is that the next step position in formation is known beforehand, and then a proper reference value is estimated and added to input reference [19]. Such method is introduced in form of equation to add a close-loop zero in transfer function while remained latent root. The forward shift of phase will expand bandwidth, and reduce position error and compensate the effect of mode changing.

However, the controllers described above have not tested with load disturbance. [14] presented the effect of load disturbance to the performance of the ball screw drive. PID controller is unable to compensate the existence of load on the mover. Proportional Derivative Disturbance Observer (PDOD) is used to compensate the sensitivity of the system towards load weight. Figure 2.7 shows the block diagram of the proposed PDOD controller.

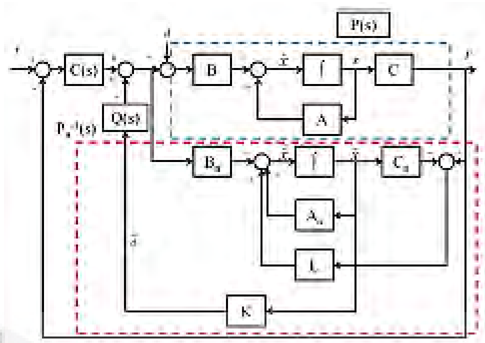


Figure 2.7: PDOP controller [14]

### 2.2.4 Synchronous Motion Control

Motion control is a vital technique for industrial machinery and semiconductor manufacturing system [7]. Motion of multiple motors must be controlled in synchronous manner. There are three categories of architectures of synchronous motion control: (a) synchronous master motion control (cross coupling technique), (b) master-slave motion control, and (c) relative dynamic stiffness motion control.

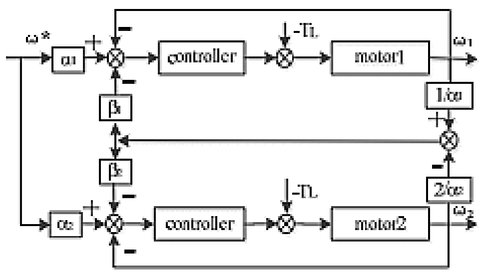


Figure 2.8: Cross-coupling motion control system [21]

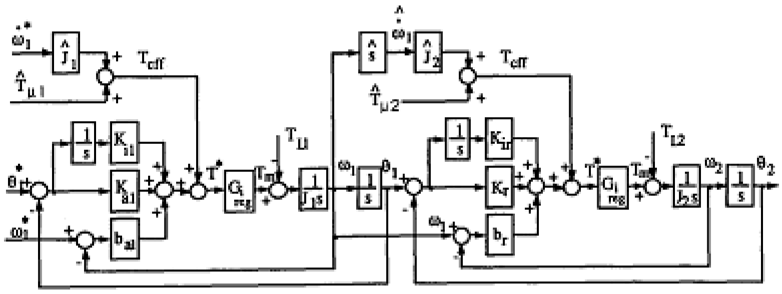


Figure 2.9: Master-slave motion control system [22]

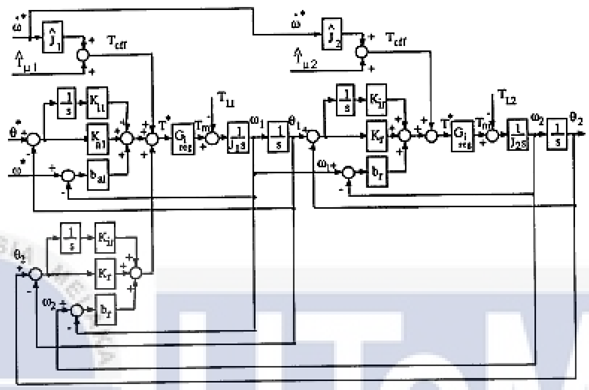

Figure 2.10: Relative stiffness motion control system [22]



In most conventional parallel controllers, no information can be received from others in the control loop of each actuator. Disturbance in a loop will result in an error which can only corrects by that particular loop only, while the others do not respond. Synchronous controller is required to address this problem.

The cross-coupling control structure of the dual-motor has the main advantage for comparing the rotational speed of two motors. Synchronization error of the rotational speed is obtained with an additional feedback signal to compensate for two motors respectively. This structure achieves better synchronization control accuracy and is suitable for two motors synchronous control as applied in [23] for dual motor networked motion control. [24] applied cross-coupling technology into common PD control architecture in parallel manipulator. The application of cross-coupling control provides solution for synchronization problem with easy and efficient implementation.

The idea of electrical cross coupling control adopted from [20], looked upon dual-axial driven system as single system contained multi-variable such as mechanical coupling effect. The cross-coupling controller is to match the counteracting of the motors toward the mechanical coupling influence.

Cross-coupling motion control is also applied in mobile robot. Most conventional controllers used in differential-drive robot consist of two individual control loops, one for each motor. In general, motion of coordination may be adjusting the reference velocities of the control loops. However, one drive loop receives no information regarding the others. [25] discussed on the cross-coupling motion controller for mobile robot and showed that the controller is very effective in compensating internal error, such as differenced in motor parameters and different bearing frictions. [26] applied cross-coupled control for all-terrain rovers by continuously comparing the wheel encoder pulses of a robot to synchronise motor speed. The result indicates improve motion accuracy by keeping the return positioning error.

On the other hand, the master-slave motion control is a well-known scheme where the slave axis receives commands from master axis. This method effectively improves the dynamic performance and system stability because the structure cannot affect the master motor [10]. This configuration reduces synchronisation error between the master and slave motors through error compensation. [5] has successfully implemented this method in ultra-precision dual stage with linear motor and Lorentz motor.

The relative stiffness motion control requires absolute loops to maintain system at virtual ground reference. Advantages of this method are estimation of acceleration of either axis is not required and less sensitive to process stiffness coupling between the axes. [22] implemented this method in dual motor drive and showed that no compromise in command tracking performance is needed.

### 2.2.5 Summary

TTDS can be actuated by servo motor or linear motor. Both motors have pros and cons in application of TTDS. Ball screw is required to translate the rotary motion generated by servo motor into linear motion. Thus, mechanical coupling is installed to attach the ball screw with shaft of the servo motor. Mover is also attached with ball screw for thrust force and linear guide to ensure straight motion. A lot of mechanical couplings are involved resulting different type of frictions. Considerations are made when modelling a system for better design of controller to compensate with these problems. However, the controller design for TTDS will not be discussed in this report. Although there are problems, ball screw drive system shows remarkable performance in ultra-high precision and less sensitive to load parameter.

Linear motor type TTDS, has no other mechanical couplings except the contact of mover with linear guide. Thus, less friction needs to be considered. However, the system is sensitive to load parameter. Changes in load easily affect the system modelling which reduces the performance. This project uses DC servo motor as less sensitive to load parameter, provides reliable control and affordable. Ease of controlling is better than linear motor. From all the researches above, modelling of the system is a necessity before the controller designing. The purpose of this step aims to determine the design specifications of the system. Then, controller can be designed to compensate the problem in order to achieve the design specifications. Mathematical modelling of the system is discussed in the next section.

## 2.3 Mathematical Modelling

Mathematical modelling is the basis of addressing control problem via control strategies. System dynamic equations can be performed analytically or numerically. The equations of motion are commonly derived from free body diagram referred to Newtonian method [27]. Free body diagram normally uses to generate equation of motion.

However, ball screw inhibits nonlinear behaviour that affecting the positioning performance. In real time application, the mass of the workpiece varies, resulting in dynamics system with time-varying parametric uncertainties [28]. Hence, different types of model are presented such as lumped model [14], friction model [29], and hybrid model [30].

### 2.3.1 Lumped model

Series Elastic Actuator (SEAs) were depicted as a simple mass-spring-damper when first introduced. Single lumped sprung mass, $m_k$ is the combination of motor rotor and transmission inertias and treated as all are moving together. Such representation is referred to as the “lumped model” in the literature [31].

[14] applied this method in modelling ball screw mechanism as shown in Figure 2.11,

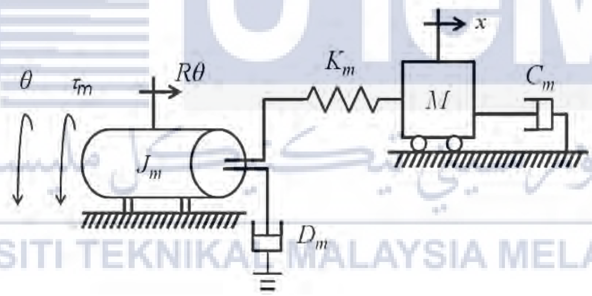


Figure 2.11: Free body diagram of ball screw diagram [14]

where $J_m$ is motor inertia in kg$m^2$, $D_m$ is motor viscous friction in Nm/rad/sec, $K_m$ is rotational stiffness of screw shaft in N/m, M is mass of table in Kg, R is transmission ratio of rotary to linear motion in m/rad and $C_m$ is viscous friction applied by mass in N/m/sec.

The equations of motions are obtained to form the dynamics model. The final dynamics model obtained is as in (2.7) and its structure is presented in Figure 2.12. The parameters are obtained through experiment.

$$\begin{bmatrix} J_m s^2 + D_m s + R^2 K_m & -RK_m \\ -RK_m & Ms^2 + C_m s + K_m \end{bmatrix} \begin{bmatrix} \theta \\ x \end{bmatrix} = \begin{bmatrix} T_m \\ f_d \end{bmatrix} \tag{2.7}$$

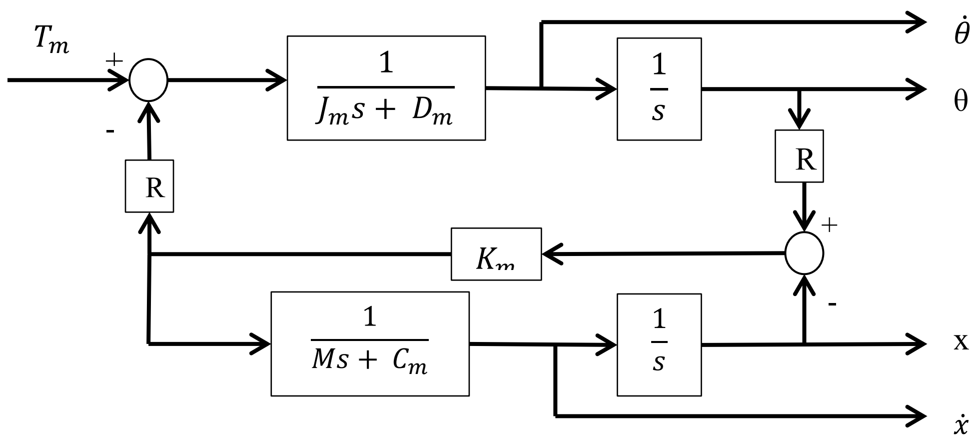


Figure 2.12: Block Diagram of ball screw mechanism [14]

[17] also applied free body diagram based on lumped model in order to obtain the equation of motion of mechanically coupled parallel ball screws. In this free body diagram, the friction is neglected and principle of superposition is applied to construct the system as two types of thrust can be added directly with the inconsideration of nonlinearity as shown in Figure 2.13, and the block diagram of single axis ball screw mechanism is shown Figure 2.14.

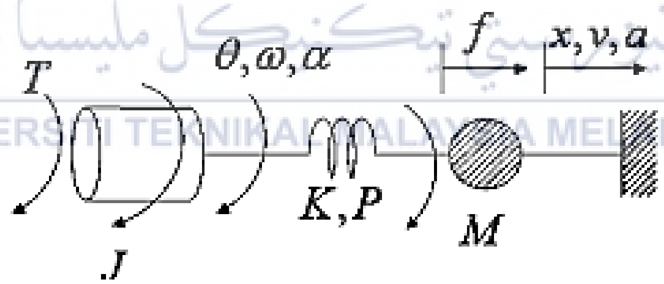


Figure 2.13: Free Body Diagram of Single Axis Ball Screw Mechanism [17]

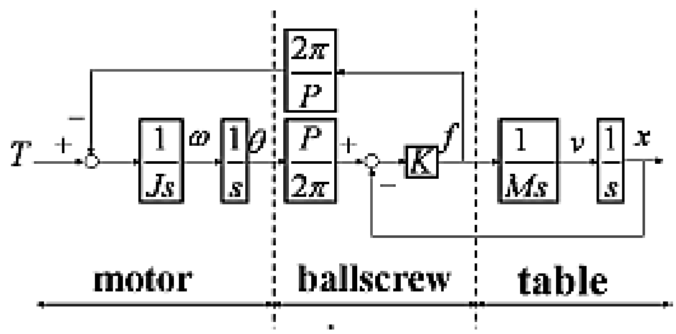


Figure 2.14: Block Diagram of Single Axis Ball Screw Mechanism [17]

The coupled system is treated as a single system because the two motors jointly drive the same stage. The relationship of velocity and subsystems is

$$\begin{bmatrix} v_1 \\ v_2 \end{bmatrix} = \begin{bmatrix} x_{11} & x_{12} \\ x_{21} & x_{22} \end{bmatrix} \tag{2.8}$$

where $x_{11}$ represents transfer function of torque input to velocity for subsystem 1 and $x_{22}$ is for subsystem 2, $x_{12}$ represents transfer function of subsystem 2 torque input to subsystem 1 velocity output and $x_{21}$ is the vice versa. The system model is presented in Figure 2.15.

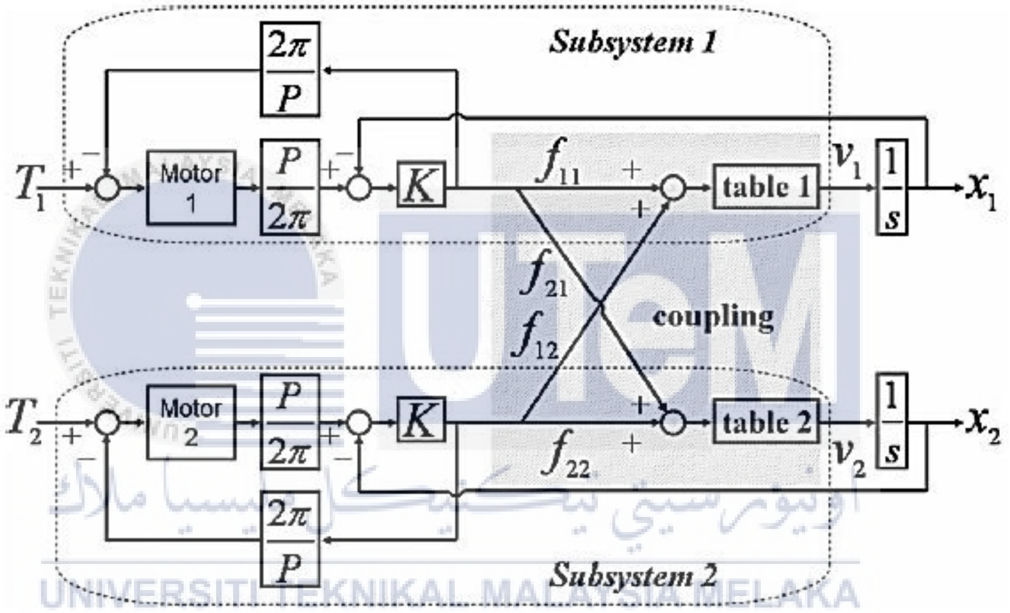


Figure 2.15: Block Diagram of Twin Axis Ball Screw Mechanism [17]

where $f_{11}$and $f_{22}$ define direct thrust of two subsystem respectively and $f_{12}$ and $f_{21}$ define the coupling effect whereby $f_{21}$ represents thrust acting on table 2 but transferred from subsystem 1 via coupling while $f_{21}$ is vice versa. The including of coupling effect in the system will improve the performance of the system [9].

The development of system model via identification technique is shown in Figure 2.16. The variable $x_{11}$ is obtained by feeding subsystem 1 with torque command $T_1$ and measuring velocity output of Table 1, and velocity output of Table 2 can also be measured to obtain$x_{12}$. $x_{22}$ and $x_{21}$ are also obtained by the same procedure. Only one motor is needed to be actuated while the other is passive. The transfer function can be obtained from the bode plot.

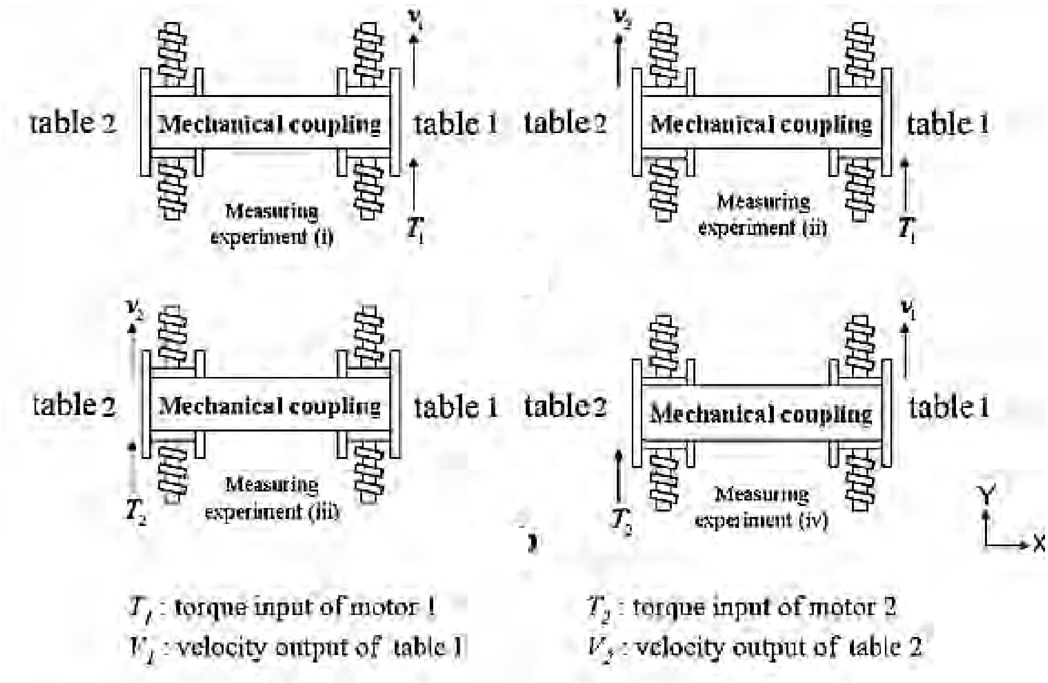


Figure 2.16: Procedure of Identification [17]

### 2.3.2 Friction model

Friction is a nonlinear phenomenon exhibits in the ball screw actuators where the force is resisting the motion of an object moving relatively to another. Motion occurs when force applied is sufficient to overcome friction. Friction model consists of three components; nonlinear term for example static, and coulomb friction, Stribeck effect, and linear term for example viscous friction [32]. Tustin and LuGre models are best to describe the friction characteristics [8, 32, 33].

In Tustin model, the effect of static friction behaves like coulomb friction, viscous friction and Stribeck effect. Coulumb friction is force that acts in the direction opposite to motion with a constant magnitude. The force acts between the two layers in contact is proportional to the sliding velocity is viscous friction. The Stribeck effect or Stribeck friction is situation when at lower velocities the friction force decreases continuously with the increase in velocity. Stiction is the maximum friction force that exists just before sliding.

Tustin model applied in [32] for modelling of nonlinear friction of the ball screw system are given by

$$F = F_n + f_v v \tag{2.9}$$

$$F_n = \left(F_c + (F_s - \ F_c)e^{-\left|\frac{v}{v_s}\right|}\right) x \ sgn(v) \qquad (2.10)$$

where $v$, $v_s$ $F_s$, $F_c$, $f_v$ and $sgn(.)$ are the table velocity, the Stribeck velocity, the maximum static friction force, the coulomb friction force, the viscous friction coefficient and signum function respectively. The identification procedure is done by inserting a sinusoidal signal to the ball screw system and the results are tabulated to obtain the value of the parameters. The same procedure is used in [8].

LuGre model describes the pre-displacement of important dynamic friction behaviour. The model is

$$\frac{d_z}{d_t} = v - \frac{\sigma_0 |v| z}{g(v)} \qquad (2.11)$$

where $v$ is the velocity relative to two contact surfaces, $\frac{d_z}{d_t}$ is the average bristle deflection, z is the bristle deflection or internal state variable, $\sigma_0$ is the brittle stiffness and $g(v)$ is the Stribeck function.

### 2.3.3 Hybrid model



Hybrid model overcomes the limitation of lumped model that degrades the dynamic performance from increasing the acceleration and lead screw slenderness ratio.

[34] developed a novel hybrid-modelling approach to describe the high frequency characteristics of ball screw drive system. The free body diagram of the lead screw is combined with motor, and the elastic distortion of the lead screw is relative to the motor rotation. Torsional and longitudinal elastics of the lead screw are considered. The hybrid model of the ball screw drive is showed in Figure 2.17 with the combination of lumped model.

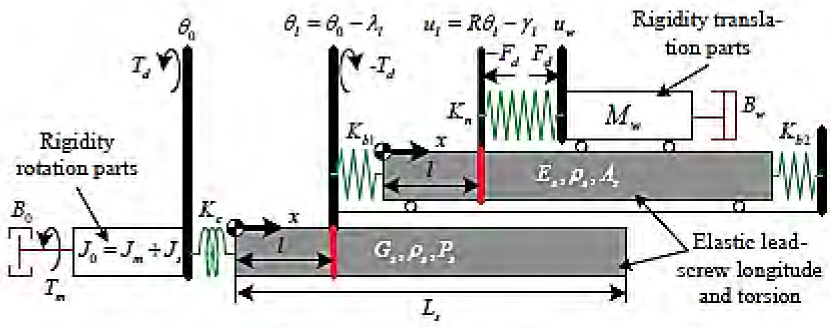


Figure 2.17: Hybrid model of ball screw drive [34]

### 2.3.4 Summary

The lumped model will be used to describe the dynamic characteristics of the system. A lot of effects are considered to model the ball screw in other model methods so lumped model is suggested to be used. Frequency response function will be used to model the parameters.

## 2.4 Frequency Response

Frequency response method (FRM) is a very practical and important alternative approach to analyse and system design. The frequency response of a system is defined as the steady-state response of the system to a sinusoidal input signal. The sinusoid is a unique input signal, and the resulting output signal for a linear system, as well as signals throughout the system, is sinusoidal in the steady state; it differs from the input waveform only in amplitude and phase angle.[35]. The FRM has the ready availability of sinusoidal test signal for various ranges of frequencies and amplitudes. This is the most reliable and uncomplicated method for experimental analysis of a system due to the ease in experimental determination of the system's frequency. The second advantage of FRM is the replacement of s with *jw* in the system transfer function *T(s)* and obtaining the transfer function describing the sinusoidal steady-state behaviour of a system.

FRM is used to determine the first axial vibration mode which was identified by an open loop frequency domain test in order to dampening out the dynamic variation caused by the structural vibration of ball screw system [28]. Besides, the determination of the resonance frequencies can also be done via FRM and used for feedback controller designing [36] with input of sinusoidal swept signal and measured the output of angular velocity.

As for system identification purpose, FRM has used to obtain the parameter of the dynamics system of the ball screw [37]. The result the parameter is then can be used to generate the transfer function of the system. The FRM can be done using dynamic signal analyser [9] with the added of a swept sine wave to the system and the resultant signal is fed back to the channel of the analyser. Bode plot of the system can be obtained via frequency response analyses and curve fitting.

Another approach of using FRM is proposed [27] with the use of MATLAB GUI in modelling the rotatory inverted pendulum. The GUI can be used to estimate the mathematical model of the system. The system is excited using band-limited white noise while the input and output of the system are collected using Micro-box. Transfer function of the system is estimated using the GUI. With the result obtained by FRM, validation is done to compare the transfer function obtained with experimental setup to ensure the modelling could represent the system model.

Hence, FRM is very convenient to be used to obtain the transfer function of a system given the advantages stated above. Approach of using MATLAB seems easier to analyse the FRM. However, there is another approach is required to collect the data of the system before the analysis of FRM.

# CHAPTER 3

# METHODOLOGY

## 3.1 Introduction

This chapter presents the organisation of the proposed project. Detail procedure and methods are described in order to achieve the objectives stated in Chapter 1. This chapter provides the general flow of this project from the initial stage to final stage.

Detail of each project procedure is organised in a project methodology flow chart. The extension of this chart is to ensure all the works are listed clearly and executed systematically. Next, a series of experiments are designed to evaluate the performance of the designed system. All the necessary information of each experiment will be listed and illustrated.

The designed system consists of hardware and software. Both parts require different type of components. The hardware components focus on selection of linear motor, linear guide, and linear encoder.. Selection of those components will be discussed in this chapter.

### 3.2 Project Flow Chart

Figure 3.1 shows the overall process to complete the proposed TTDS project. The flow includes information gathering, fabrication, purchasing, and experimental tests. These steps are further explained in the next sections.

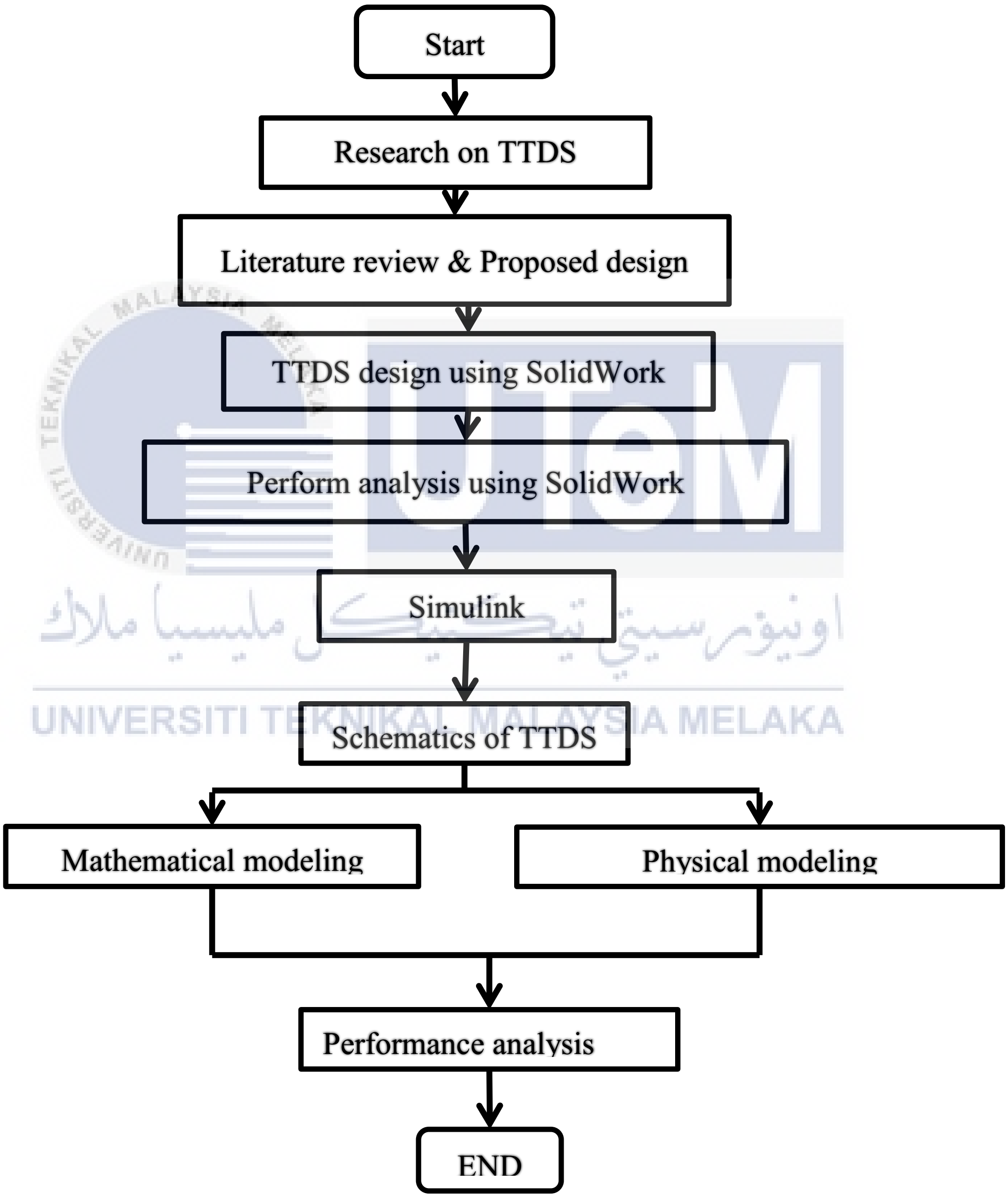




Figure 3.1: TTDS project flow

## 3.3 Project Methodology Flow Chart

Figure 3.2 overviews the contents discuss in chapter 3 which includes the procedure to design and model the TTDS.

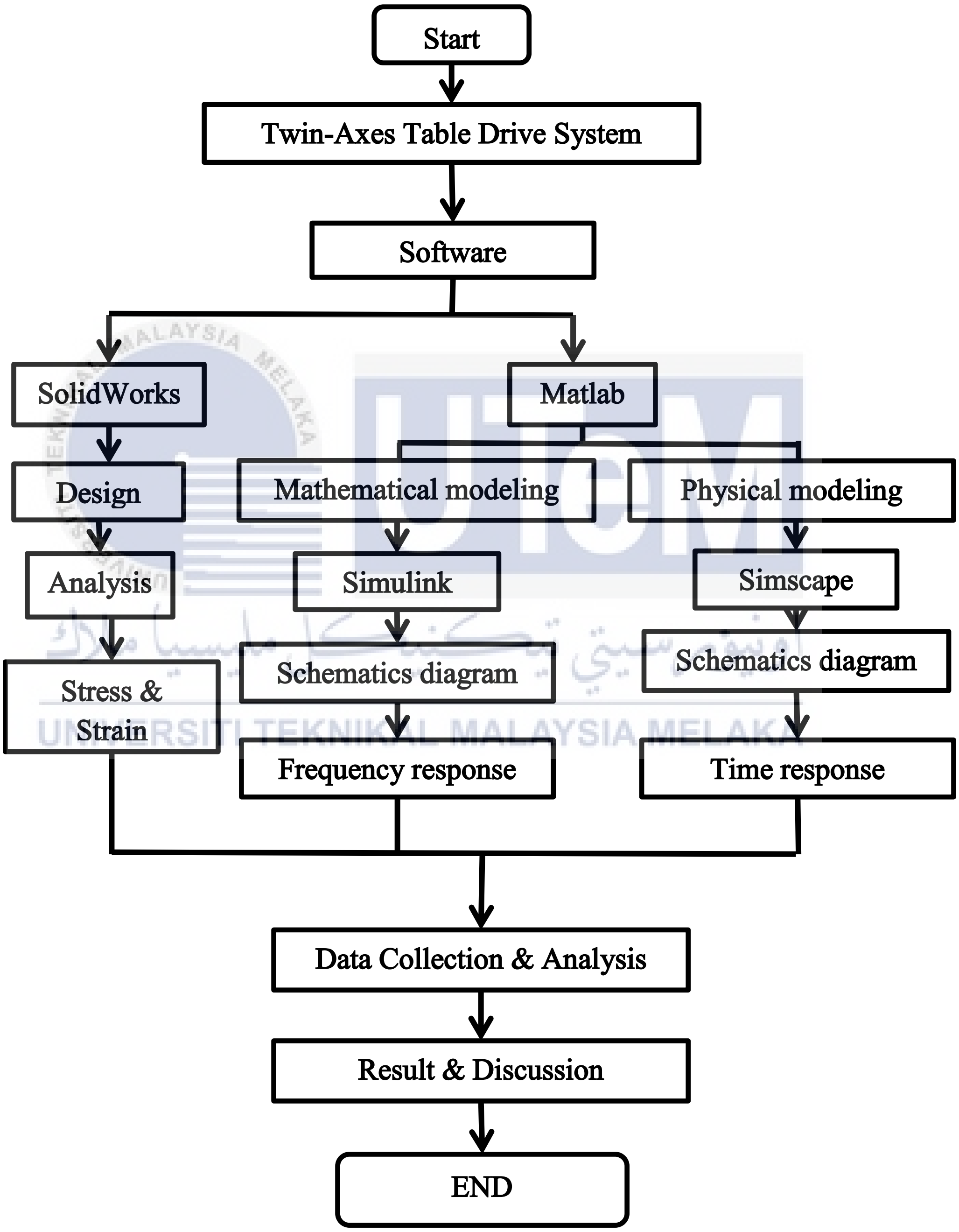


Figure 3.2: TTDS project methodology flowchart

## 3.4 TTDS Component Description

### 3.4.1 TTDS Base Structure

Base structure is the foundation to support the construction of the TTDS components. All the components of TTDS will be installed on to the base as shown in Figure 3.3. This base has the dimension of 350mm x 250mm.

Figure 3.3: TTDS base structure [38]

### 3.4.2 Linear Guide and Mover

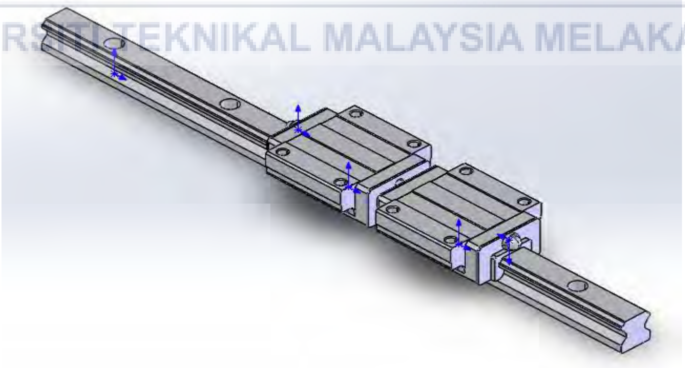

Figure 3.4: Linear guide and mover

Moreover, mover plays an important role to carry load. In TTDS, both ball screw units are separated in a distance of 50mm. The diagram of the mover is illustrated in Figure 3.4. Linear guide ensures the motion of the motor is in a straight line. A linear motor cannot operate without guidance. Furthermore, the tolerance air gap between the linear motor and track must always remain constant to ensure maximum performance.

Linear guide is used with mover in this project. This mover is moulded with rollers to reduce the number of components in TTDS.

### 3.4.3 Linear Motion Actuator

Actuator generates motion. In TTDS, there are two actuators that are rotary motors. Rotary motors generate rotary motion either in clockwise or counter clockwise. Thus, ball screw mechanism is needed to translate the rotary motion into linear motion.

The advantage of DC servo motor is the ease in speed and positioning control. However, this motor must be equipped with sufficient torque to carry the load of 10Kg. DC servo motor RS-263-6011 is used in the proposed TTDS, Figure 3.5 and Table 3.1 shows the motor and its specification respectively.



Figure 3.5: DC servo motor RS-263-6011 [39]

Table 3.1: Specification

| Specification | Unit |
|---|---|
| **Maximum Output Torque** | 36 Ncm |
| **Supply Voltage** | 24-30 Vdc |
| **Output Speed** | 1600 rpm |
| **Power Rating** | 30 W |
| **Stall Torque** | 12Ncm |
| **Shaft Diameter** | 6mm |
| **Length** | 88mm |
| **Width** | 66mm |

The motor is coupled with ball screw. The ball screw acts as translator from rotational motion to linear motion. The diameter of the ball screw is 8mm with the length of 325mm as shown in Figure 3.6. The combined motor and ball screw is shown in Figure 3.7.

Figure 3.6: Ball screw [40]

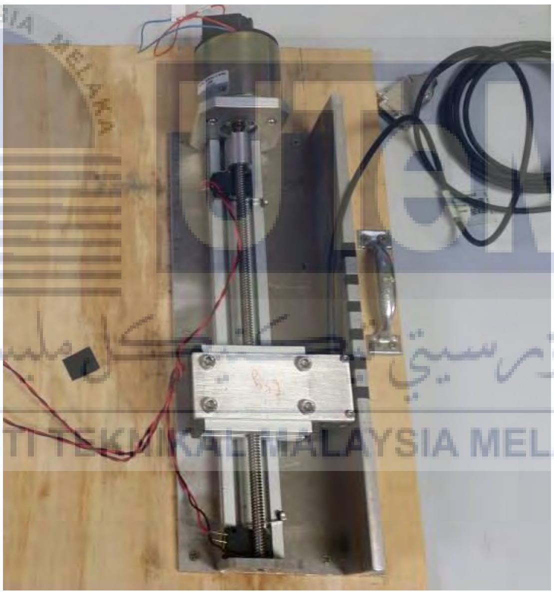



Figure 3.7: Single unit ball screw system

### 3.4.4 Linear Encoder

Encoder acts as position recognition of either rotary or linear motion. Linear encoder detects the position of current object when senses linear motion.

RGH22A30L00A is chosen as linear encoder in the proposed TTDS position recognition. However, the encoder chosen is only a readhead and a tape scale is needed for the scale reading purpose. RGS scale is suitable for readhead RGH22A as shown in Figure 3.8.


Figure 3.8: Linear encoder readhead RGH22A [41]

The readhead has analogue output signal with 1Vpp differential, equipped with incremental type. Figure 3.9 below shows the specification of the readhead.

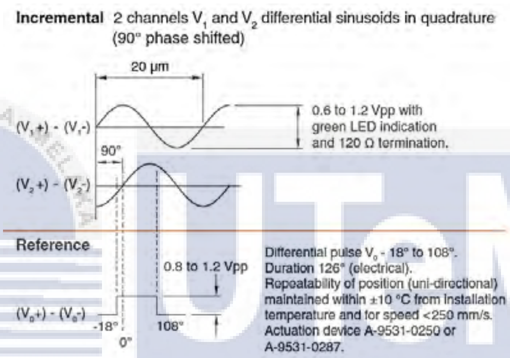


Figure 3.9: Specification of RGH22A [41]



## 3.6 Hardware Simulation and Analysis

### 3.6.1 TTDS Hardware design

This step aims to illustrate the complete TTDS design before fabrication and assembly. SolidWorks is used to design the TTDS hardware. All parts stated in previous section are illustrated with the purpose to design the TTDS and are drawn in SolidWorks. Each part is in separate file. An assembly file combines all the parts use to construct the TTDS. The whole TTDS will be viewed in orthographically.

### 3.6.2 Mover Stress Simulation

The stress simulation is used to analysis the stress test of the large mover with the maximum of 10 kg weight. Analysis will show the capability of the large mover to carry the load in term stress experienced on mover. Tools needed are SolidWorks and SolidWorks simulation.

Only the large file with large mover is required for the stress test. New study is executed for new simulation and select the material used to manufacture the mover.

<u>Procedure</u>

1) Aluminium is selected as the material of mover.
2) Fixture is determined by selecting the model surface.
3) Load is applied to a particular area means for analysis with the correct insertion of the gravitational force.
4) Mesh is created to ensure all parts are in contact to each part. Error will occur when there are parts intersect to others.
5) „Continue‟ is pressed and „Stress, Displacement, and Safety factor‟ will be displayed with colours. Only result of stress is analysed.
6) Load weights to be tested are 2kg, 4kg, 6kg, 8kg, and 10kg.



## 3.7 System Modelling

The TTDS is the combination of two units of single axis ball screw systems. The aluminium plate is acting as the mechanical couple which bridges two ball screw drive systems. From previous research, a convenience way has been used [9] where “subsystem” is named for each ball screw with driving motor. Thus, “subsystem 1” and “subsystem 2” distinguished the two units respectively. The “stage” is used to name over whole system.

This section presents the identification procedure for modelling of TTDS via simulation. Firstly, effort is done on constructing the block diagram of TTDS for the modelling purpose. Such block diagram is constructed based on the parameters from past research.

### 3.7.1 Past Research

The past research [14] has constructed a single ball screw system as shown in Figure 3.10(a) and the construction of the ball screw system is shown in Figure 3.10 (b). The free body of the single ball screw system is shown in Figure 2.11 and the equation of motion is presented in equation (2.7). Details calculation of the equation of motion is given in Appendix A. The block diagram of the ball screw illustrated in Figure 2.12 based on the lumped model.

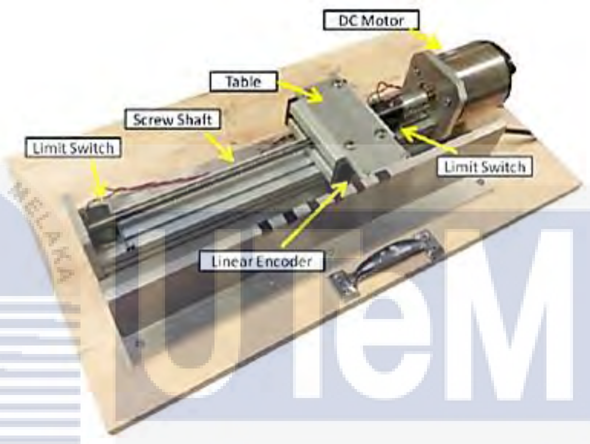


(a)

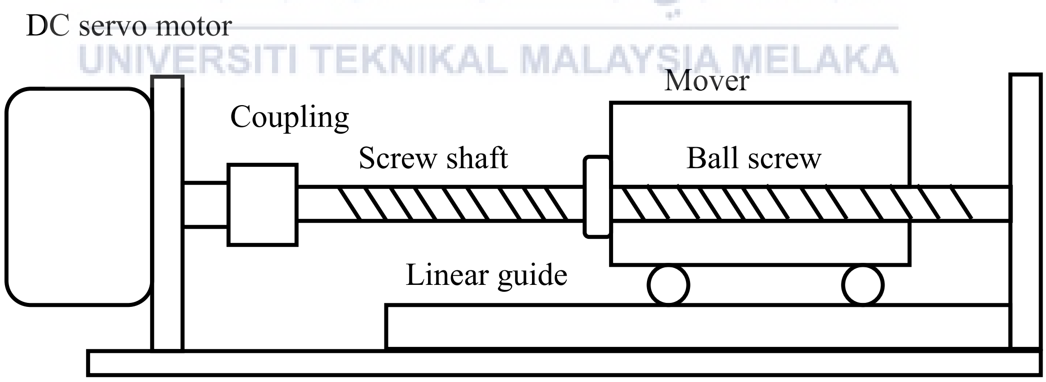


(b)

Figure 3.10: Single axis ball screw system [14]



A DC servo motor; RS Component: RS 263-2011, is used to drive the ball screw, with 0.09 Vs/rad of back electromotive force constant. The motor is driven by a voltage amplifier with voltage gain of 2 and input voltage to the amplifier is limited to ± 10V. The ball screw is measured as 8 mm/rev with a maximum range of 160mm.

The displacement of the system is measured by a linear encoder; Renishaw: RGH22A30L00A, with resolution of 5µm. The sampling frequency used in the experiment is set as 1 kHz [14]. The measured parameters of the motor are showed in Table 3.2. The single axis ball screw system which is the reference system is used to simulate the TTDS. The block diagram of the single axis ball screw system is illustrated in Figure 3.11. On the other hand, the block diagram of TTDS is shown in Figure 3.12.

Table 3.2: Parameters of the DC servo motor

| Parameter | Description | Value | Unit |
|---|---|---|---|
| $Jm$ | Motor Inertia | $6 \times 10^{-5}$ | $kgm^2$ |
| $D_m$ | Motor Viscous Friction | $3.85 \times 10^{-4}$ | Nm/rad/s |
| $K_m$ | Rotational stiffness of screw shaft | $1.82 \times 10^{3}$ | N/m |
| $M$ | Mass of mover | $5 \times 10^{-1}$ | kg |
| R | Transmission ratio of rotatory to linear motion | $1.273 \times 10^{-3}$ | m/rad |
| $C_m$ | Viscous friction applied by mover | $5 \times 10^{1}$ | N/m/s |
| $L_m$ | Motor inductance | $5 \times 10^{-3}$ | H |
| $R_m$ | Motor resistance | 7.8 | Ohms |
| $K_b$ | Back electromotive force constant | $9 \times 10^{-2}$ | Vs/rad |



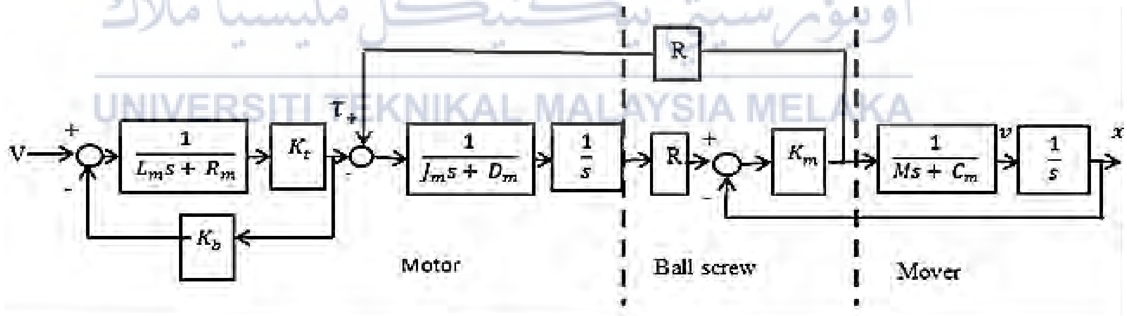


Figure 3.11: Block diagram of single axis ball screw system [14]

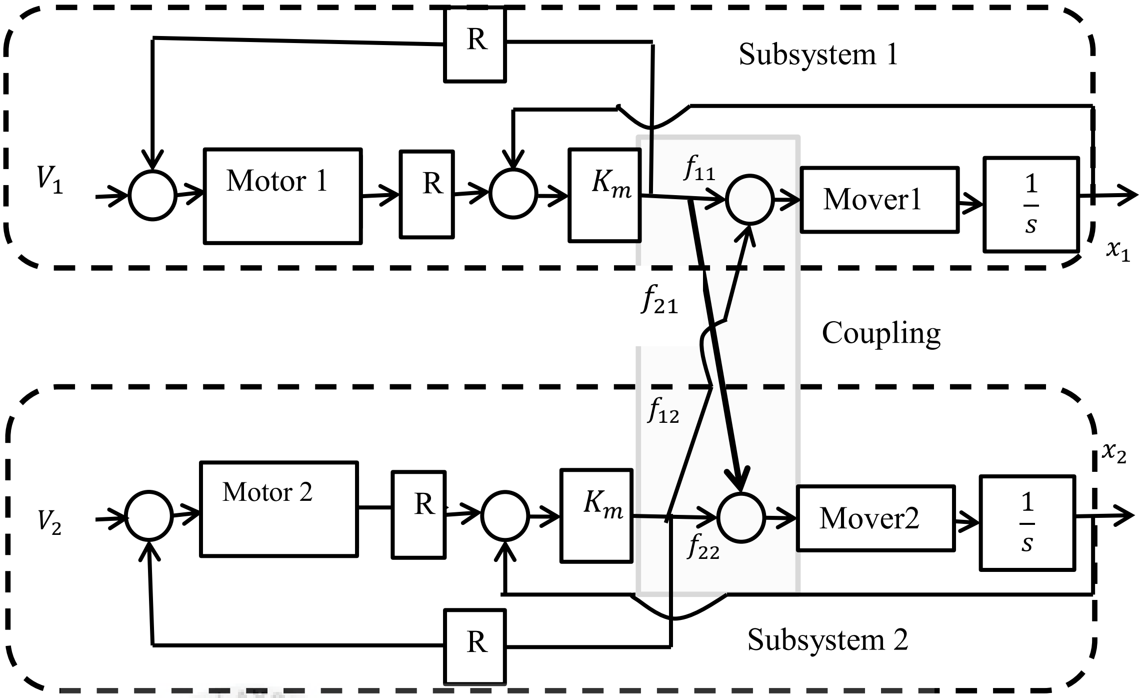


Figure 3.12: Block diagram of the reference system of TTDS [9]

### 3.7.2 Simulated System

The free body diagram of the single axis ball screw driven system are modelled based on lumped model. Three assumptions for the lumped model are made: one side of the actuator is treated as the output with the other side serving as ground, the motor and transmission inertias are combined into a single lumped inertia and the actuator dynamics are derived with the motor torque as the input and the force on the assumed output side as output [31].

Using the frequency response method, a second order transfer function of single ball screw system will be generated. The parameters of the ball screw system are lumped together as shown in Figure 3.13 with voltage input, V, and displacement output, x. The descriptions of the parameters are described in Table 3.3. Thus, the transfer of the ball screw is

$$Z(s) = \frac{X}{V} = \frac{k_t}{s[(J_s+B)+ k_b k_t]} \tag{3.1}$$

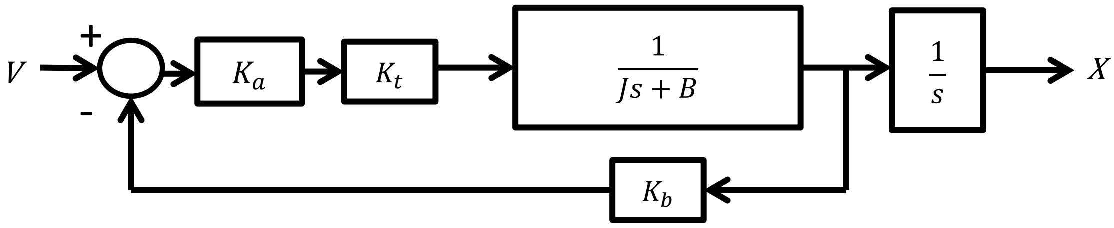


Figure 3.13: Second order ball screw drive table [14]

Table 3.3 Parameter of lumped model ball screw drive table

| Symbol | Parameter |
|---|---|
| V | Voltage input |
| J | Effective inertia of ball screw, motor and load |
| B | Effective damping coefficient of ball screw, motor and load |
| X | Displacement |
| $K_a$ | Amplifier gain constant |
| $K_t$ | Motor constant |
| $K_b$ | Back electromotive force constant |



### 3.7.3 Modelling of Coupled System

The “mover” as illustrated in Figure 3.14 is the part where the two balls are interacted through the coupling for TTDS. The coupled system is treated as a single unit because the both motors are driving the same mover. The relationship between the two ball screws is shown in Figure 3.14 with voltage input to the system and velocity output. $V_1$ is the voltage input to motor 1 and $V_2$ is for motor 2. $f_{11}$ and $f_{22}$ represent the voltage input of two subsystem acting on movers respectively. $v_1$ and $v_2$ define the velocity output of respective subsystem. $f_{12}$ and $f_{21}$ represent the coupling effect where $f_{12}$ is the thrust acting on mover 2 but transferred from subsystem 1, meanwhile the $f_{21}$ is the thrust transferred from subsystem 2 through the coupling.

For simplification, the relationship of the system

$$\begin{bmatrix} v_1 \\ v_2 \end{bmatrix} = \begin{bmatrix} x_{11} & x_{12} \\ x_{21} & x_{22} \end{bmatrix} \begin{bmatrix} V_1 \\ V_2 \end{bmatrix} \tag{3.2}$$

From (3.2), $x_{11}$ represents the transfer function of the velocity output to voltage input of subsystem 1, and $x_{22}$ is that for subsystem 2. $x_{12}$ represents the transfer function of the voltage input of subsystem 2 to velocity output on subsystem 1 and $x_{21}$ is the reverse direction

An identification technique [9] is used for the system identification to construct the system model as shown in Figure 3.14. This method is simulated where the subsystem 1 is fed with voltage input $V_1$, and the velocity output of mover 1 is measured as shown in Figure 3.14 (A), the transfer function $x_{11}$ can be obtained. At the same time, the velocity output is also measured to determine $x_{21}$. The procedure to obtain $x_{22}$ and $x_{12}$ is the same but this time the voltage input is given to subsystem 2 as shown in Figure 3.14 (B). The data is analysed through algorithms to obtain the transfer functions.

Only one motor is allowed to be actuated while the other should be left completely passive when performing identification procedures. The mover is not easily moved by ball screw. Hence, a close loop identification technique for TTDS is performed to address this problem. Before the identification procedure, both motors and ball screws are fed with a sine wave voltage input of constant frequency. This step aims to start the two motors at the same low frequency to ensure the mover of the passive ball screw can be easily be dragged by the actuated motor for measurement. The velocity feedback loop is included to stabilize the system.

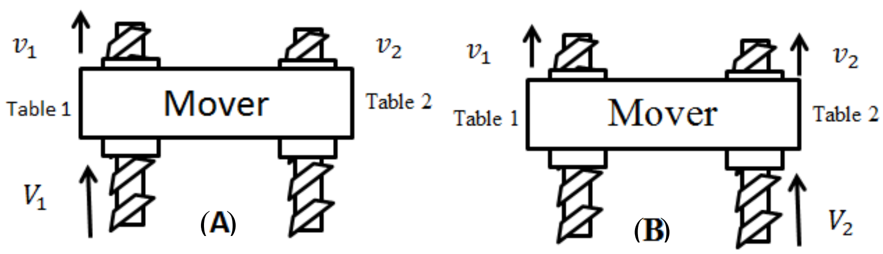


Figure 3.14: Identification procedure. (A): velocity output of both systems system are measured with voltage input at subsystem 1; (B): Velocity output of both systems system are measured with voltage input at subsystem 2

The two motors and ball screws are started for 5 seconds with the frequency of 0.8rad/s. Sine wave with frequency of 1 rad/s is given as voltage input to one motor. Note that, only one motor is actuated in the identification process at one time. This step is repeated for the input frequencies from 1.2 rad/s to 30 rad/s with the interval of 0.2 rad/s. The maximum frequency of 30 rad/s is inserted to the system is due the natural frequency of the reference system is 29.1 rad/s. The output velocity of both subsystems is recorded using Transfer Function (TF) algorithm. This method is able to determine the coupling effect in both directions. The transfer functions can be obtained via frequency response using *iddata* command in Matlab.

Based on the above identification procedure, the simulation is conducted using the block diagram of single ball screw shown in Figure 3.11 and the parameters in Table 3.2. The TTDS is constructed with the assumption that both subsystems have identical parameters and for the coupled system, the coupling is the shaded region shown in Fig 3.12.

Procedure to compare the transfer functions obtained from coupled and uncoupling system is as follow. The two subsystems are identified separately with the disassembled of the coupling. Hence, each model represents the characteristics of each individual subsystem. The system can be described as

$$\begin{aligned} v_1 &= x^*_{11} * V_1 \\ v_2 &= x^*_{22} * V_2 \end{aligned} \tag{3.3}$$



Open-loop test is performed to validate the performance of the transfer functions obtained with the reference system. An input voltage of 1 V is fed to the both models and the velocity output is measured.

## 3.8 Physical Modelling of TTDS

The physical modelling of TTDS can be constructed using Simscape. Simscape enables the creating of physical systems rapidly within the Simulink environment. Simscape can build physical component models based on physical connections that directly integrate with block diagrams and other modelling paradigms. Besides, the development of control system, testing of the system-level performance and customisation of the component model can be conducted,.

The construction of TTDS consists of three parts which are motor, ball screw, and mover as shown in Figure 3.10 (b). The physical modelling of the single axis ball screw system is illustrated in Figure 3.15 and modelling of all the parts are shown in Appendix C. The construction of physical modelling of the TTDS in is shown in Figure 3.16. Both subsystems of the TTDS are assumed to be identical.

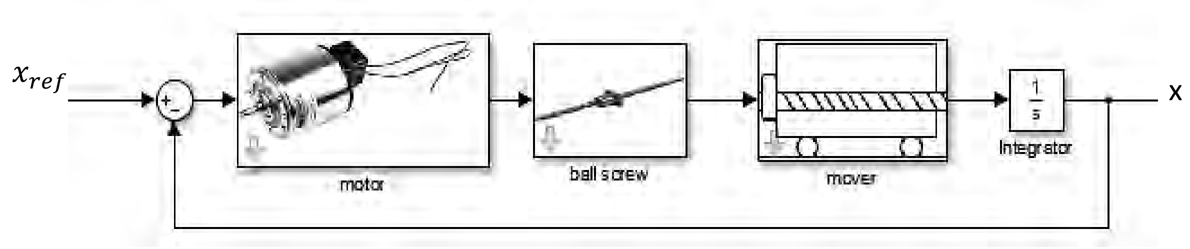


Figure 3.15: Physical model of single ball screw system

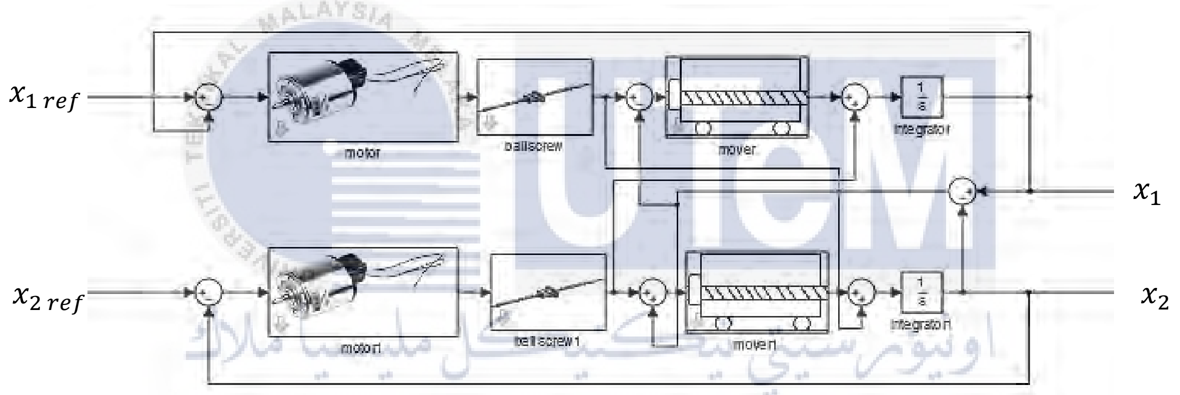


Figure 3.16: Physical model of TTDS



The performance of the single axis ball screw system in Figure 3.15 and TTDS in Figure 3.16 are compared with varying the load. In this experiment, only the load of the mover is manipulated to simulate the load weight to be driven. Different load of 2kg, 4kg, 6kg, 8kg, and 10kg are applied with the same input reference displacement of 1mm. In the single ball screw system, the total load is inserted to the parameter of the mover but the total load to be driven is divided by half in the case of TTDS for each subsystem of the mover respectively. This is due to be principle of moment whereby the load is assumed located at the centre of the large mover. The step response of the TTDS is tabulated and plotted for each experiment. Note that the reference single ball screw system is only capable to drive the maximum load of 5 kg. Hence, the load can only be double to 10kg for TTDS.

# CHAPTER 4

# RESULT AND DISCUSSION

## 4.1 Overview

This chapter presents the results from the experiments described in chapter 3. Discussions include the hardware design, stress test analysis, free body diagram, and dynamics characteristics equations of TTDS.

## 4.2 SolidWorks Analysis

### 4.2.1 TTDS Hardware Design

The design of TTDS is drawn and displayed in orthographic views as shown in Figure 4.1, Figure 4.2, Figure 4.3, and Figure 4.4.



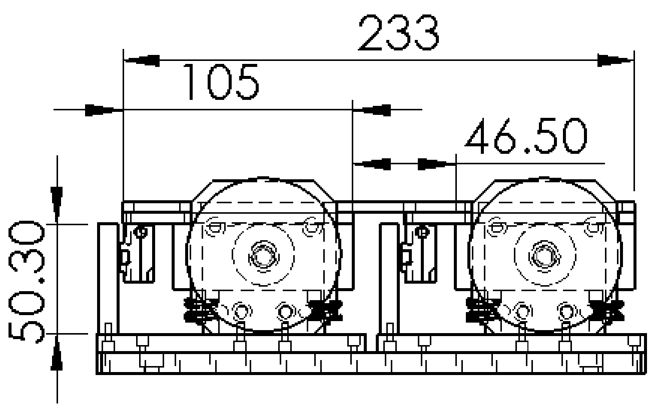


Figure 4.1: Front view

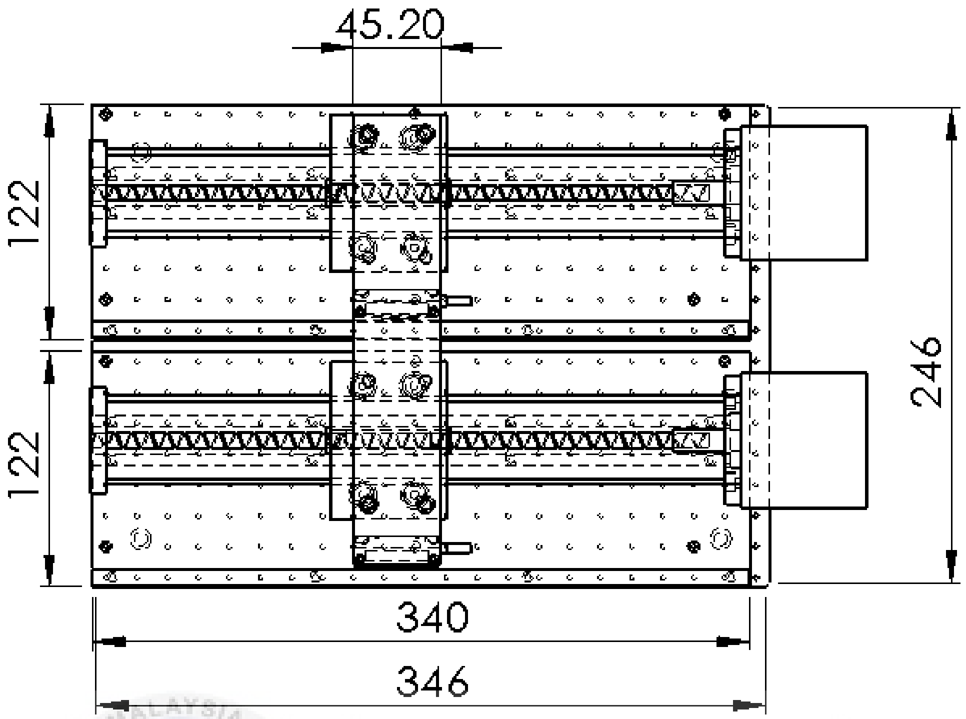


Figure 4.2: Top view

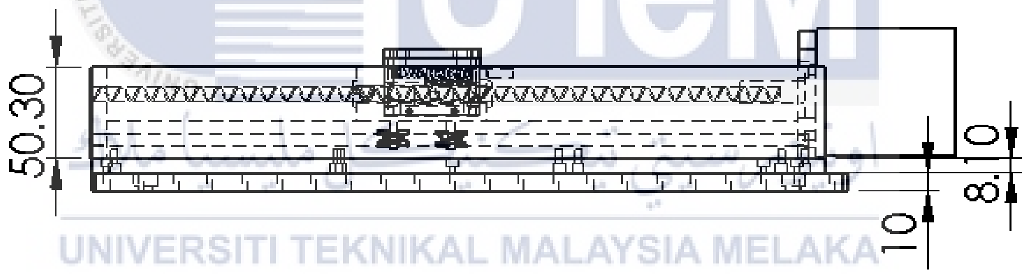




Figure 4.3: Side view

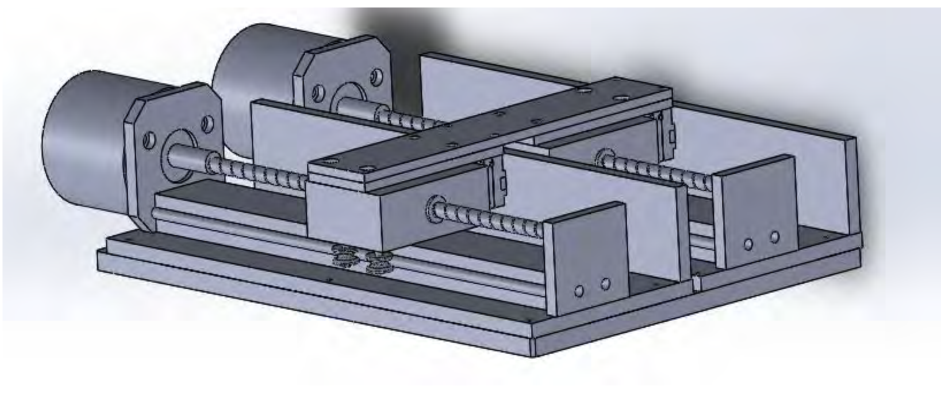

Figure 4.4: Overall design of TTDS

### 4.2.2 Stress and Strain Analysis

The parameters used for this simulation are:

1) Material – Aluminium
2) Thickness: 5 mm
3) Width: 223 mm
4) Length : 45.2 mm
5) Material : Aluminium
6) Distance between axis : 46.5 mm
7) Yield strength: 5.515x10^8 N/m^2
8) Weight: 15g

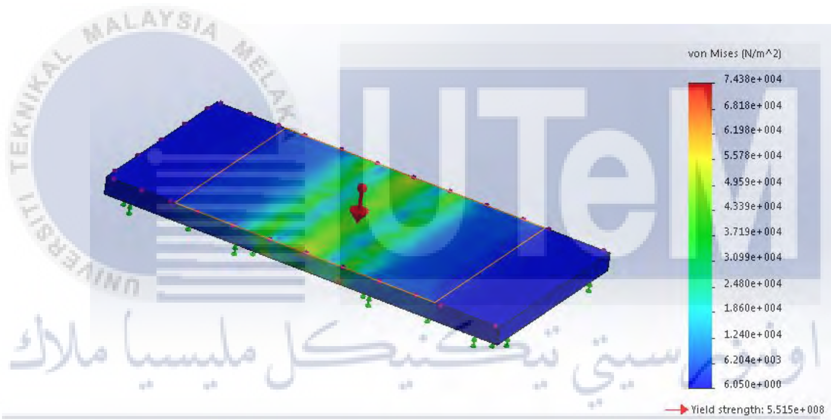


Figure 4.5: Preliminary result on stress test of large mover

The load is placed within the red colour line. Stress experienced by the mover is indicated by colours. Red colour means the stress is near to the yield strength of the aluminium. The result of the analysis is tabulated in Table 4.1 and plotted in Figure 4.6.

Table 4.1: Result of stress test

| Load, kg | Stress, N/m^2 |
|---|---|
| **2** | 1402 |
| **4** | 4445 |
| **6** | 6089 |
| **8** | 8753 |
| **10** | 11830 |

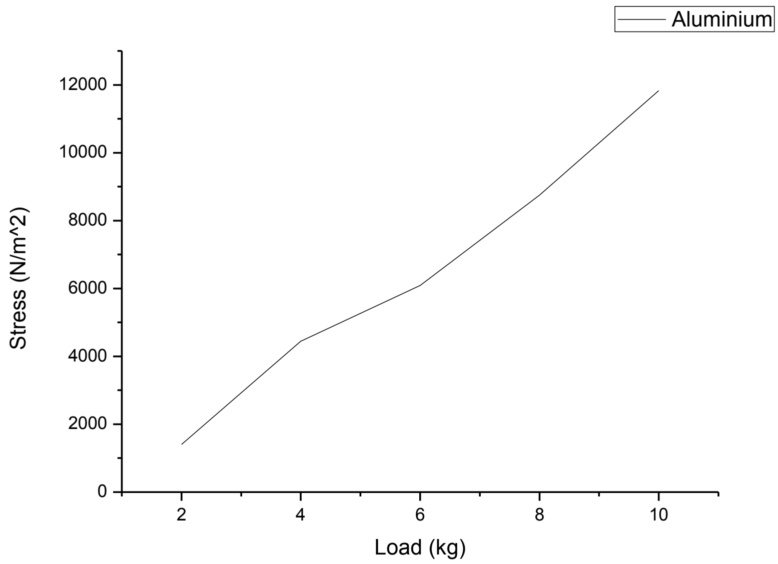


Figure 4.6: Stress test on aluminium type large mover

Figure 4.6 shows that the stress experienced by the mover is proportional to the load weight. However, aluminium has the yield strength of 5.515x10^5 N/m^2 and the stress experienced by the mover when carrying the maximum weight of 10 kg is 0.1183 x10^5 N/m^2.

The analysis indicates that the large mover with the dimension of 223 mm x 45.2 mm x 5 mm is capable of carrying mass of 10kg without breaking. This mover is suitable for the proposed TTDS.



## 4.3 System Modelling

The frequency response method is used to obtain the transfer functions of the TTDS as described in section 3.2 and 3.3. The result of the transfer function of coupled model is illustrated in Figure 4.7. Only the transfer function for the uncoupled model will be discussed.

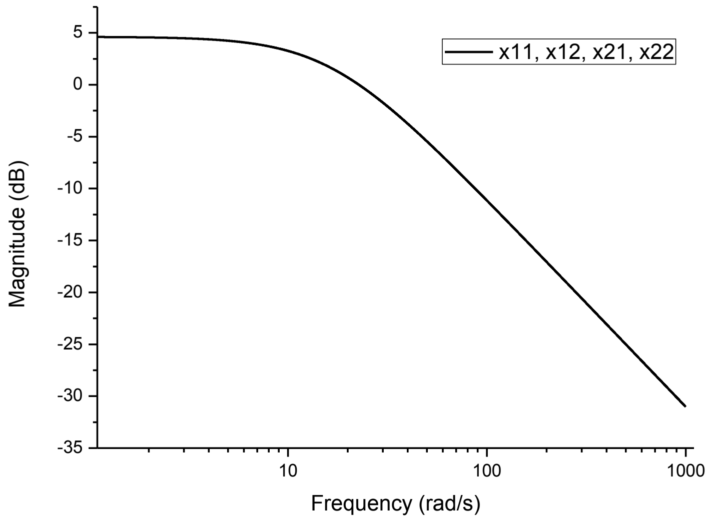


Figure 4.7: Bode plot of TTDS

The transfer functions for $x_{11}$, $x_{12}$, $x_{21}$, and $x_{22}$ are obtained by plotting of the Bode plots as shown in Figure 4.7. The result obtained for all these four transfer functions are the same which is

$$x_{11} = x_{12} = x_{21} = x_{22} = \frac{28.1}{s+16.5} \tag{4.1}$$

As for the uncoupled model, the two individual subsystems have the transfer functions as shown in

$$x^*_{11} = x^*_{22} = \frac{58.458}{s+17.11} \tag{4.2}$$

The result shows that the uncoupled system has the same order of system as shown in Fig 4.7 but different transfer function. This is due to the different steps performed during the identification procedure. Only the velocity output of the subsystem with voltage input is measured at one time. Note that the aluminium mover is still attached for both the modelling cases during the identification procedure. The validation of the transfer functions for the coupled model with the reference system is shown in Figure 4.8 with the error of the performance shown in Figure 4.9.

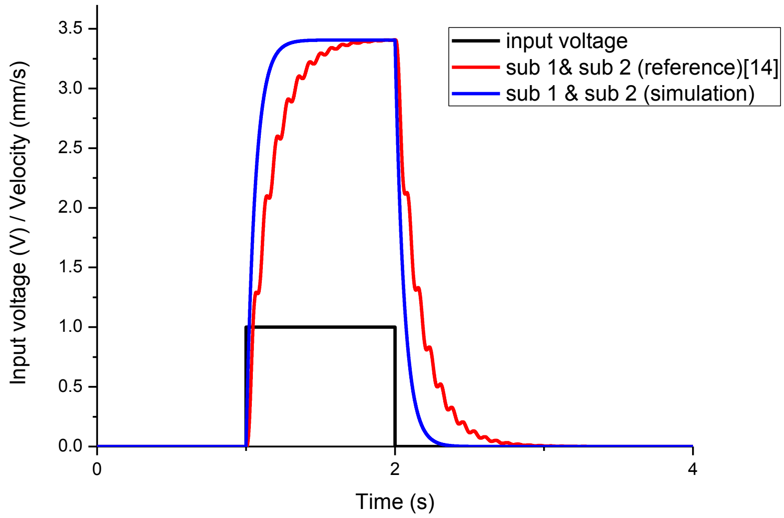


Figure 4.8: Comparison of velocity curve for the reference system and simulated system

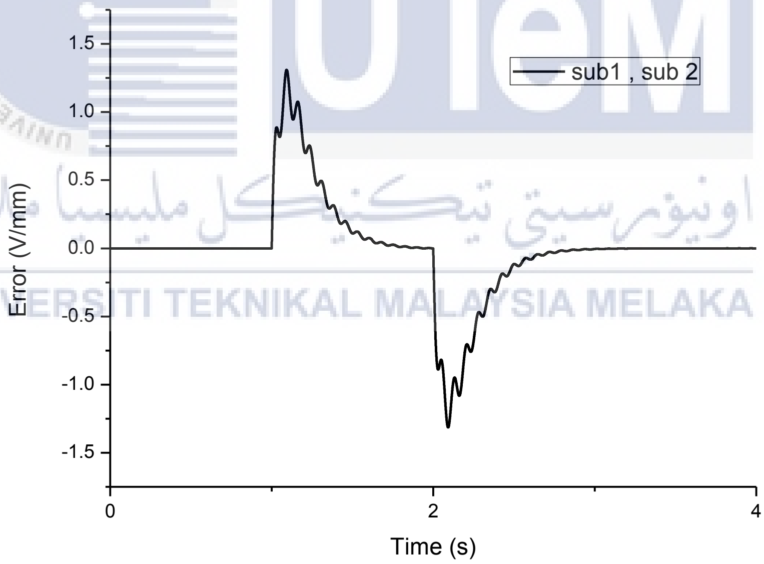


Figure 4.9: Error of velocity displacement of the reference system with the transfer functions.

Figures 4.8 and 4.9 show that the transfer functions have the performance with the maximum error of 1.3 V/mm. The comparison is done by taking the error of the voltage velocity of the reference system with the transfer functions obtained. These transfer functions can be used for future researches in the TTDS.

## 4.4 Physical Modelling

The physical modelling of the TTDS and single ball screw system are tested with varying load from 2kg to 10kg via simulation. Each increment made in load is 2kg. The step responses of the system are illustrated in Figure 4.10 and 4.11 for the lightest load and the heaviest load respectively. The others step responses are showed in Appendix B.

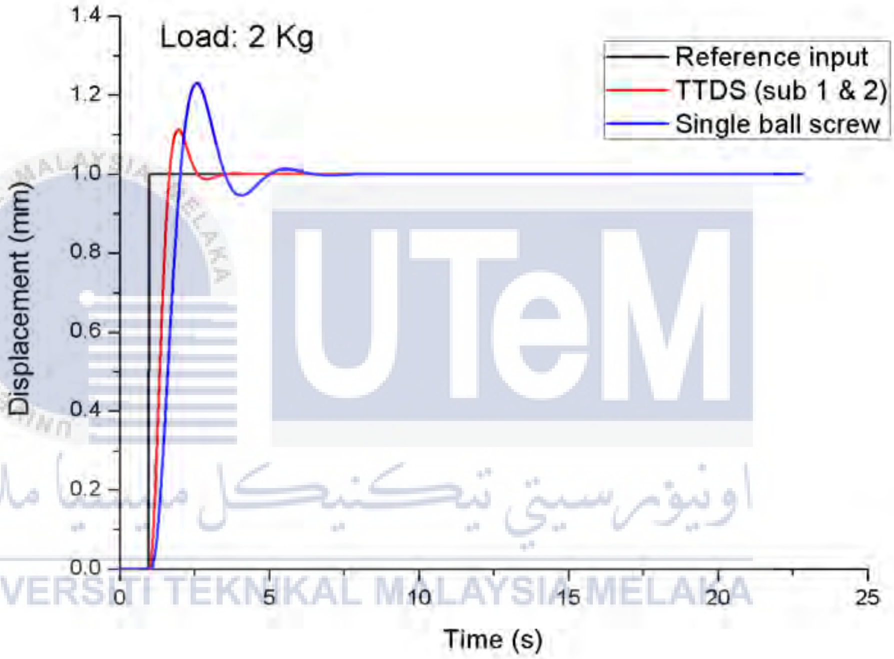


Figure 4.10: Step response of TTDS with reference input of 1 mm and 2 kg of load.

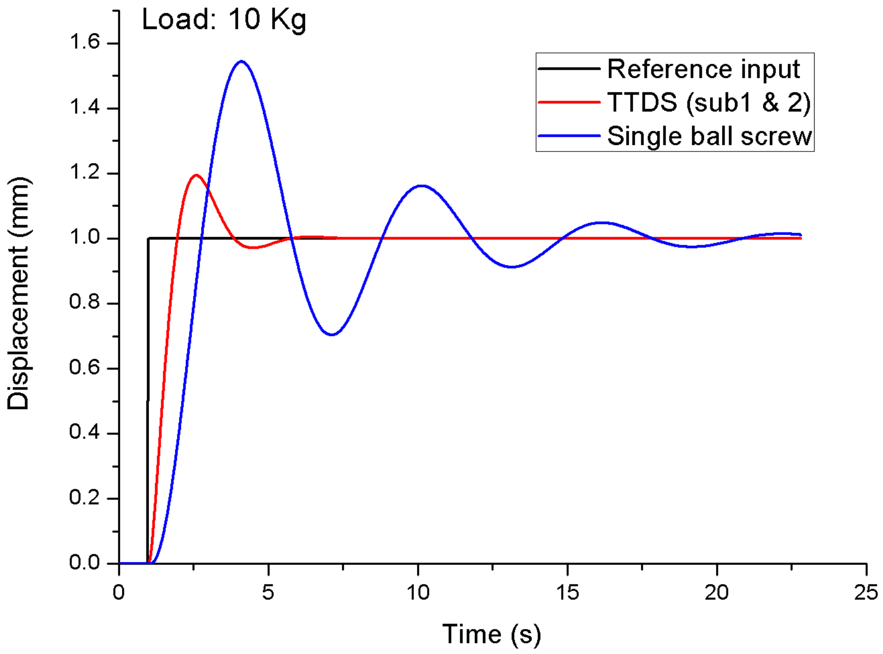


Figure 4.11: Step response of TTDS with reference input of 1 mm and 10 kg of load.

Table 4.2: Transient response of TTDS and single ball screw system

| **Load, Kg** | **2** | | **4** | | **6** | | **8** | | **10** | |
|---|---|---|---|---|---|---|---|---|---|---|
| | TTDS | Single | TTDS | Single | TTDS | Single | TTDS | Single | TTDS | Single |
| **Rise time, s** | 0.444 | 0.65 | 0.516 | 0.78 | 0.58 | 0.909 | 0.63 | 0.633 | 0.675 | 0.71 |
| **Peak time, s** | 1.957 | 2.57 | 2.16 | 3.06 | 2.36 | 3.454 | 2.46 | 3.79 | 2.584 | 4.1 |
| **Settling time, s** | 2.9 | 4.81 | 3.715 | 9.02 | 4.28 | 12.29 | 4.65 | 17.39 | 5.04 | 20.01 |
| **Overshoot, %** | 11.1 | 22.84 | 17.1 | 36.3 | 18.45 | 46.3 | 19.8 | 108.7 | 19.9 | 110.68 |
| **Peak value, mm** | 1.11 | 1.23 | 1.168 | 1.371 | 1.187 | 1.451 | 1.19 | 1.504 | 1.194 | 1.54 |

From Table 3, the settling time, peak time, and overshoot of the single ball screw system shows increment as the weight is heavier. The overall response of single ball screw table drive system is slower when the load weight to be driven increased to 4 Kg and become unstable when driving load more than 4 kg. However, TTDS is still capable to maintain the tracking performance for varying load weight of 10 Kg.

## 4.5 Summary

This chapter presents the design of the TTDS in SolidWorks. The stress test is carried out on the aluminium type large mover with 10 Kg of load. The result shows that the mover can withstand the load. Modelling starts by presenting the free body diagram of the TTDS. Single axis ball screw presents the mechanical parts and free body is presented. The transfer functions of the TTDS of coupled and uncoupled models are obtained via frequency response. Moreover, validation for the transfer function of the coupled model TTDS is done via simulation with the reference system. TTDS is also constructed in physical model where the performance of the TTDS is compared with single axis ball screw system with varying load.

# CHAPTER 5

# CONCLUSION AND FUTURE WORK

## 5.1 Conclusion

The main focus of this project is to construct and mathematically model the Twin-Axes Table Drive System (TTDS). Details methodologies are presented in the project and project methodology flow charts. Starting point of this project is information gathering on related previous studies on TTDS. Rotary motor is used in for the design of TTDS this project because the performance and reliability of this type of motor for TTDS has been proven.

The TTDS is designed with two motors and two ball screws which are used to drive a large mover. Studies have showed that the synchronous control of TTDS is still a major problem and hence, system model is essential to design suitable controller to compensate the problem. However, the controller design is not covered in the project. A reference system is constructed based on past research. An identification procedure is conducted to obtain the transfer function of the TTDS using coupled model via frequency response. The obtained transfer functions can perform as the reference system with acceptable error using open loop test via simulation. This identification procedure has proven that this method can be used to test the system under stable condition.

The performance of the TTDS and single ball screw system with varying load is done via simulation. The result shows that TTDS can perform better than the single ball screw system for 2 kg to 10 kg load.

## 5.2 Future Work

Future work includes the performing of the identification procedure stated above to obtain the transfer function of the TTDS experimentally. Open loop test can be performed experimentally to validate the obtained transfer functions. Moreover, the extension to the research is the controller designing for the TTDS to address the synchronous problem by identifying the design specifications through the dynamic characteristics of the system.

The physical model of the TTDS can be used to evaluate the performance of the system by performing different types of tests. Tests can be varied in term of specification of the motor, ball screw, and load to be driven. These tests are to ensure the performance of the system is as expected or acceptable before any modification to the system.

**REFERENCES**


[1] Ha-Joon Chang,"The manufacturing sector and the future of Malaysia‟s economic development" in Management Journal 2012, 2012, pp.4-12.

[2] Dr. Ariff, "Malaysia Growth Experience" , May 2015 [Online]. Available: http://yangon.sites.unicnetwork.org. [Accessed: 8-Nov-2017].

[3] Terasaki, Fumio, Jun Kobayashi, Ryuichi Oguro, and Fujio Ohkawa. "A Positioning Control of a Serial Twin Linear Slider System with Machine Stand Vibration." In Industrial Technology, 2006. ICIT 2006. IEEE International Conference on, pp. 2925-2930

[4] Tsuruta, Kazuhiro, Tetsuya Ojiro, and Hideki Honda. "Synchronization control for twin-axes table drive system." In Industrial Electronics Society, IECON 2015-41st Annual Conference of the IEEE, pp. 005162-005167.

[5] Hou, Bo-jie, Jian-she Gao, and Yun-fei Zhou. "The development of an ultra-precision dual-stage based on a master-slave control system." In Computer Distributed Control and Intelligent Environmental Monitoring (CDCIEM), 2012 International Conference on, pp. 727-730.

[6] Hsieh, Min–Fu, and Wei–Che Chang. "Combining full and semi closed loop synchronous control for dual mechanically coupled ball screw system." International Journal of Computer Applications in Technology 45, no. 2-3 (2012): 139-147.

[7] Mao, Wei-Lung, Jyun-Cheng Huang, and Jen-Wei Lin. "Design of synchronized control method of dual-axis linear actuator." In Consumer Electronics-Taiwan (ICCE-TW), 2015 IEEE International Conference on, pp. 456-457.

[8] Niranjan, Prabha, Shwetha C. Shetty, Chaithra D. Byndoor, K. V. S. S. S. S. Sairam, and Shashikanth Karinka. "Friction identification and control of ball screw driven system using PLC." In Recent Trends in Electronics, Information & Communication Technology (RTEICT), IEEE International Conference on, pp. 803-808.

[9] Min-Fu Hsieh, Wu-Sung Yao, and Chia-Rong Chiang, “Modelling and synchronous control of single-axis stage driven by dual mechanically-coupled parallel ball screws”, in It J Adv Manuf Tehnol (2007), pp. 934-943

[10] Zhang, He, Baoquan Kou, and Chaoning Zhang. "A new position loop stiffness testing method for linear motor servo systems." In Electrical Machines and Systems (ICEMS), 2015 18th International Conference on, pp. 498-502.

[11] Kiyoshi Ochi, and Masami Saeki, “Coaxial control for injection equipment by twin ball screw drive”, in The 47th IEEE International Midwest Symposium on Circuits and Systems 2004. pp. III-145- III-148.

[12] Zhang, Chengyong, and Yaolong Chen. "Tracking Control of Ball Screw Drives Using ADRC and Equivalent-Error-Model-Based Feedforward Control." IEEE Transactions on Industrial Electronics 63, no. 12 (2016): 7682-7692.

[13] Dong, Liang, and Wencheng Tang. "Control of ball screw drives using adaptive backstepping sliding mode controller and minimum tracking error prefilter." In Control & Automation (ICCA), 11th IEEE International Conference on, pp. 995-1000.

[14] Jia En Foo, Shin Horng Chong, Wai Keat Hee, Ser Le Loh, and Norhaslinda Hsahim, “Fast positioning performance in ball screw mechanism with disturbance observer”, in Jurnal Technology (Science & Engineering), 2016. pp. 71-78.

[15] Junicjiro Yuno, Kenichi Nakanishi and Manabu Sawada, “Development of servo motor driven workpiece gripping device”, in SICE Annual Conference 2017, Sept 19-22 2017. pp. 961-966.

[16] Linear mechanism, “ Unites States Naval Academy” [online]. Available: https://www.usna.edu/EE/ee301/supplements/Linear%20Motors%20Supplement.pdf. Accessed: 18-Nov-2017.

[17] R. C. Okonkwo; R. Hanitsch, “Development and control of a prototype permanent-magnet DC linear motor”, in IFT Electric Power Applications, 2007, volume 1. pp. 223-228.

[18] Kazuhiro Tsuruta; Tetsuya Ojiro; Hideki Honda, “Synchronization control for twin axes table drive system”, in IECON 2015 - 41st Annual Conference of the IEEE Industrial Electronics Society,Year: 2015. pp. 005162 – 005167

[19] Imen, S. J., and M. Shakeri. "Feed forward adaptive control of a linear brushless DC motor." In SICE, 2007 Annual Conference, pp. 2200-2204.

[20] Dongmei Yu; Qingding Guo; Qing Hu; Jiang Lili , “Position synchronized control of dual linear motor servo system using fuzzy logic”, in 6th World Congress on Intelligent Control and Automation, 2006, volume 2. pp. 8041-8044.

[21] Kazuhiro Tsuruta; Tetsuya Ojiro; Hideki Honda, “Synchronization control for twin axes table drive system”, in IECON 2015 - 41st Annual Conference of the IEEE Industrial Electronics Society,Year: 2015. pp. 005162 – 005167

[22] Lorenz, Robert D., and Peter B. Schmidt. "Synchronized motion control for process automation." In Industry Applications Society Annual Meeting, 1989., Conference Record of the 1989 IEEE, pp. 1693-1698.

[23] He, Fang, and Chuang Wang. "Cross-coupling synchronous control of dual-motor networked motion control system." In Control Conference (CCC), 2017 36th Chinese, pp. 7628-7633. IEEE, 2017.

[24] Su, Y. X., Dong Sun, Lu Ren, Xiaoyun Wang, and James K. Mills. "Nonlinear PD synchronized control for parallel manipulators." In Robotics and Automation, 2005. ICRA 2005. Proceedings of the 2005 IEEE International Conference on, pp. 1374-1379. IEEE, 2005.

[25] Feng, L., Y. Koren, and J. Borenstein. "Cross-coupling motion controller for mobile robots." IEEE control systems 13, no. 6 (1993): 35-43.

[26] Reina, Giulio. "Cross-coupled control for all-terrain rovers." Sensors 13, no. 1 (2013): 785-800.

[27] Fong, T. Teng, Z. Jamaludin, and L. Abdullah. "System Identification and Modelling Of Rotary Inverted Pendulum." International Journal of Advances in Engineering & Technology 6, no. 6 (2014): 2342.

[28] Bao, Dafei, and Wencheng Tang. "Adaptive sliding mode control of ball screw drive system with extended state observer." In Control, Automation and Robotics (ICCAR), 2016 2nd International Conference on, pp. 133-138.

[29] Yamamoto, Takayuki, Masakazu Naito, Gan Chen, and Isao Takami. "Robust control design for ball screw system via descriptor representation and loop shaping." In Modelling, Identification & Control (ICMIC), 2014 Proceedings of the 6th International Conference on, pp. 82-87.

[30] Liu, Yan, Tong Zhao, and Hui Zhang. "Hybrid dynamic modeling of a high-speed ball-screw drive system." In Mechanic Automation and Control Engineering (MACE), 2010 International Conference on, pp. 3049-3052.

[31] Orekhov, Viktor L., Coleman S. Knabe, Michael A. Hopkins, and Dennis W. Hong. "An unlumped model for linear series elastic actuators with ball screw drives." In Intelligent Robots and Systems (IROS), 2015 IEEE/RSJ International Conference on, pp. 2224-2230.

[32] Yamamoto, Takayuki, Masakazu Naito, Gan Chen, and Isao Takami. "Robust control design for ball screw system via descriptor representation and loop shaping." In Modelling, Identification & Control (ICMIC), 2014 Proceedings of the 6th International Conference on, pp. 82-87.

[33] Niranjan, Prabha, K. V. S. S. S. S. Sairam, and Shashikantha Karinka. "Position control of single stage dual range positioning system." In Research and Development (SCOReD), 2016 IEEE Student Conference on, pp. 1-5.

[34] Liu, Yan, Tong Zhao, and Hui Zhang. "Hybrid dynamic modeling of a high-speed ball-screw drive system." In Mechanic Automation and Control Engineering (MACE), 2010 International Conference on, pp. 3049-3052.

[35] Bao, Dafei, and Wencheng Tang. "Adaptive sliding mode control of ball screw drive system with extended state observer." In Control, Automation and Robotics (ICCAR), 2016 2nd International Conference on, pp. 133-138. IEEE, 2016.



[36] Fujita, Tomoya, Atsushi Matsubara, Daisuke Kono, and Iwao Yamaji. "Dynamic characteristics and dual control of a ball screw drive with integrated piezoelectric actuator." Precision engineering 34, no. 1 (2010): 34-42.

[37] Hatwesh, Ashraf, Simon Fletcher, Andrew Longstaff, Wencheng Pan, and Fengshou Gu. "Expedient identification of the dynamics of ball-screw drives using online-validation." In Automation and Computing (ICAC), 2017 23rd International Conference on, pp. 1-6. IEEE, 2017.

[38] Baseplate, Misumi [Online]. Available: https://us.misumiec.com/vona2/detail. Accessed: 18-Nov-2017.

[39] DC servo motor RS-263-6011, specification. Available: http://docs-europe.electrocomponents.com/webdocs/1516/0900766b81516ab4.pdf. Accessed: 18-Nov-2017

[40] Ball screw, Misumi [Online]. Available: https://us.misumi-ec.com/vona2/detail/110300079220. Accessed: 18-Nov-2017

[41] Linear encoder, RGH22A series, [Online]. Available: http://www.renishaw.com/en/rgh22-incremental-encoder-system-with-rgs-linear-scale--6443. Accessed: 19-Nov-2017.

**Appendix A: Equation of motion**

The three components have respective equation s of motion.

$$J_m\ddot{\theta} + D_m\dot{\theta} + RK_m\,(R\theta - x) = \tau_m \tag{4.1}$$

$$f_c = K_m\,(R\theta - x) \tag{4.2}$$

$$M\ddot{x} + C_m\dot{x} - f_c = f_d \tag{4.3}$$

Substitute equation (4.2) into (4.3) yields equation (4.4).

$$M\ddot{x} + C_m\dot{x} - K_m\,(R\theta - x) = f_d \tag{4.4}$$

The Laplace transform of the equations (4.4)

$$(J_m s^2 + D_m s + R^2 K_m)\,\theta(s) - RK_m x(s) = \tau_m(s) \tag{4.5}$$

$$-RK_m\,\theta(s) + \;(Ms^2 + C_m s + K_m) = x(s) \tag{4.6}$$

Represent (4.5) and (4.6) in matrix form



$$\begin{bmatrix} J_m s^2 + D_m s + R^2 K_m & -RK_m \\ -RK_m & Ms^2 + C_m s + K_m \end{bmatrix} \begin{bmatrix} \theta(s) \\ x(s) \end{bmatrix} = \begin{bmatrix} \tau_m(s) \\ f_d(s) \end{bmatrix} \tag{4.7}$$

Using the Cramer"s Rule, the transfer function of the single axis ball screw TTDS is

$$\frac{x(s)}{\tau_m(S)} = \frac{RK_m}{(J_m s^2 + D_m s + R^2 K_m)(Ms^2 + C_m s + K_m) - (RK_m)^2} \tag{4.8}$$

where $f_d$ is assumed zero.

**Appendix B: Step response of TTDS with single axis ball screw system**

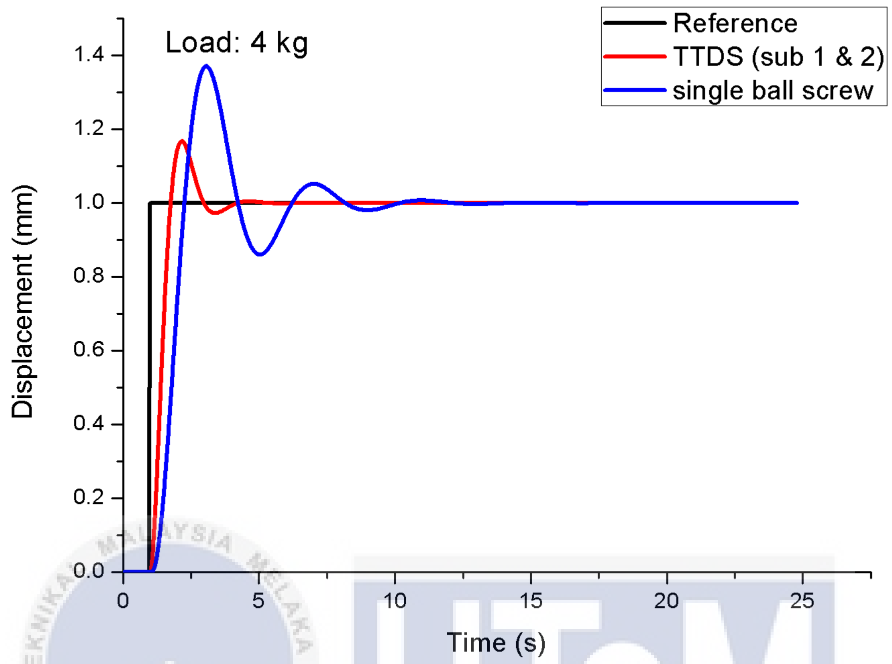


Figure B1: Step response of TTDS with reference input of 1 mm and 4 kg of load.

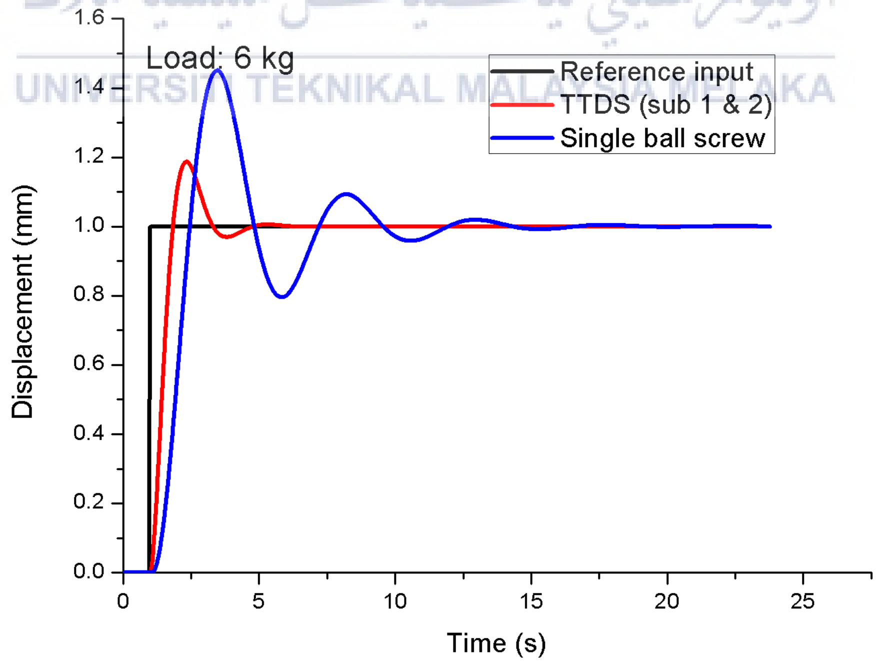


Figure B2: Step response of TTDS with reference input of 1 mm and 6 kg of load.

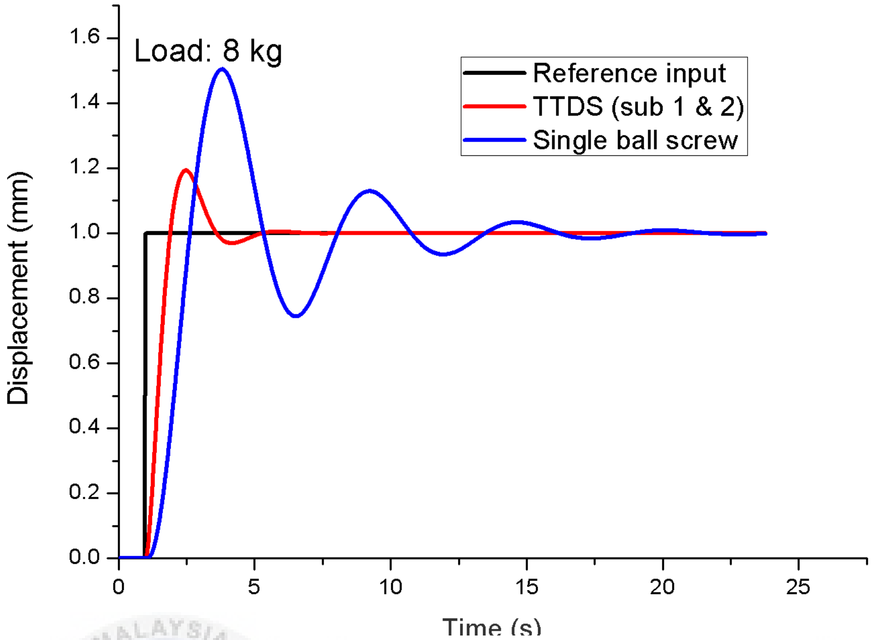


Figure B3: Step response of TTDS with reference input of 1 mm and 8 kg of load.

**Appendix C: Physical model**

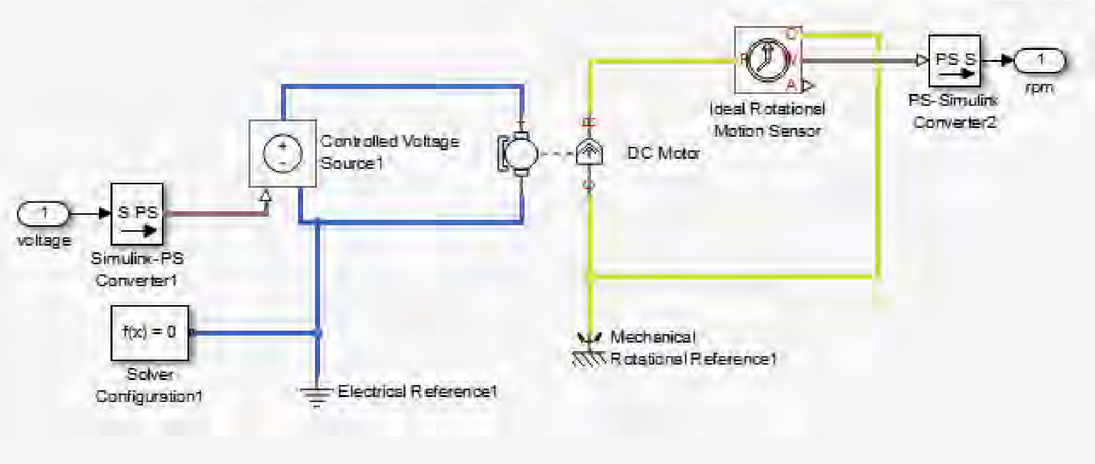


Figure C1: Physical model of motor

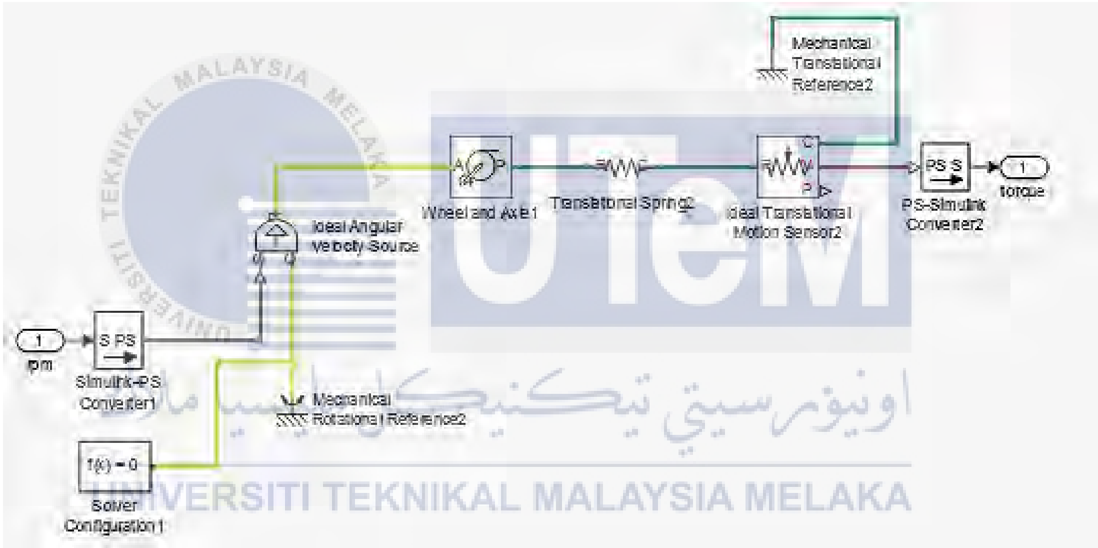




Figure C2: Physical model of ball screw

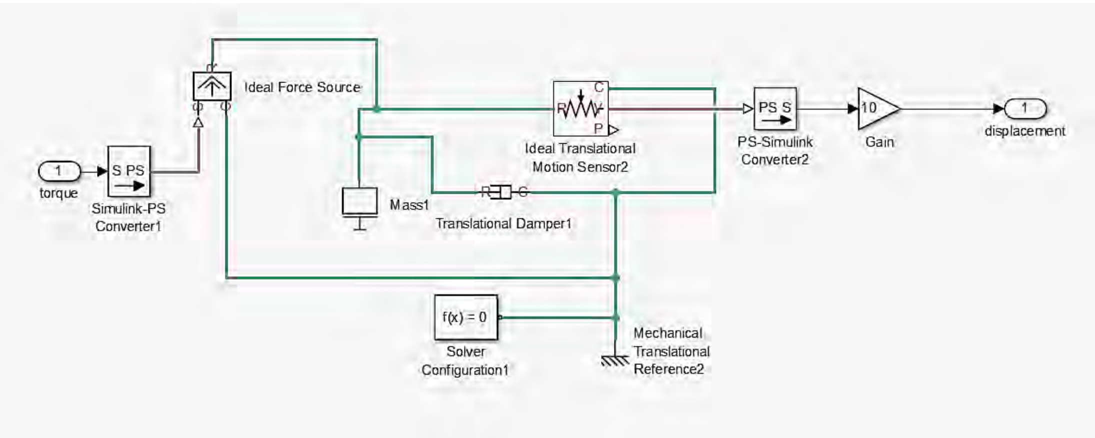


Figure C3: Physical model of mover

**Appendix E: TF algorithm**

```
% Opening Simulink
model = 'ttds';
load_system(model);
ify = 0.8;

for test=1: 1:5;

% Run Simulink
ify = ify + 0.2;
set_param([model, '/Sine Wave'],'frequency','ify');
sim(model);

% Data collection
output1=Sc(:,4);
n1output= output1(25001:end);
output= Sc(:,3);
noutput= output(25001:end);
input= Sc(:,2);
ninput= input(25001:end);
t= Sc(:,1);
x= t(25001:end);
plot (x,noutput);
hold on
% Find max value over all elements.
[peakF,peakt] = findpeaks(noutput);
time = x(peakt);
plot (x,n1output);
[peakF1,peakt1] = findpeaks(n1output);
plot(time, peakF, 'r*', ...
    'LineWidth', 2, 'MarkerSize', 10);

plot(x,ninput);
plot(time, peakF1, 'b*', ...
    'LineWidth', 2, 'MarkerSize', 10);

t1input=ninput(peakt1);
plot(time, t1input, 'm*', ...
    'LineWidth', 2, 'MarkerSize', 10);

tinput= ninput(peakt);
plot(time, tinput, 'y*', ...
    'LineWidth', 2, 'MarkerSize', 10);

% find peak value of output data
[a,b]=size(peakF);
s=sum(peakF);     % sum of all columns
total=sum(s);     % total sum
```

```
Favg=total/(a*b);

% find peak value of output data
[e,f]=size(peakF1);
s=sum(peakF1);    % sum of all columns
total=sum(s);    % total sum
F1avg=total/(e*f);

% find peak value of output data
[c,d]=size(tinput);
s=sum(tinput);    % sum of all columns
total=sum(s);     % total sum
Gavg=total/(c*d);

% find peak value of output data
[g,h]=size(t1input);
s=sum(t1input);    % sum of all columns
total=sum(s);     % total sum
G1avg=total/(g*h);


%Record data into spreadsheet
  xlApp = actxserver('Excel.Application');
  xlApp.visible = 1;

%Open the the spreadsheet
  xlworkbook = xlApp.Workbooks.Open('D:\utem\FYP\innovate\singleaxis.xlsx');
   xlsheet = xlworkbook.ActiveSheet;
  mydata= [ify Favg Gavg F1avg G1avg];
  data=xlsread('singleaxis.xlsx');

%Determine last row
  last=size(data,1);
  newRange=last+1;
  xlCurrRange = xlsheet.Range(['A', num2str(newRange),':E', num2str(newRange)]);
  xlCurrRange.Value2 = mydata;

%Save and Close the Excel File
   invoke(xlworkbook,'Save');
  invoke(xlApp,'Quit');
  delete(xlApp);
end

%Bode Plot
A= xlsread('innovate_final result_sub1');
% prepare data for tftest, 200 is a random chosen sampling time
fs= logspace (0,1.477, 150);
tfdata = iddata(A(:,2),A(:,3),0.0001, 'frequency', fs);
N = 1; % Number of poles
Z = 0;
```

```
sys = tfest(tfdata,N,Z)
[mag, phase, freq]= bode(sys,fs);
magnew=mag(:);
mag1= 20*log(magnew);
fsnew=fs(:);
phasenew=phase(:);
bodeplot(sys,fs)
```